



TALLINN UNIVERSITY OF TECHNOLOGY

SCHOOL OF ENGINEERING

Department of Electrical Power Engineering and Mechatronics

**FEM BASED MODELLING AND ANALYSIS OF
ECCENTRICITY FAULTS IN INDUCTION MOTORS**

**LÕPLIKEL ELEMENTIDEL PÕHINEV
ASÜNKROONMOTORITE EKSTSENTRILISUSE
MODELLEERIMINE JA ANALÜÜS**

MASTER THESIS

Student: Naveenraj Akkam Veetil

Student code: 194528 MAHM

Supervisor: Dr. Toomas Vaimann
Senior researcher

Co-Supervisor: Hadi Ashraf Raja
(Early stage researcher)

Tallinn 2022

AUTHOR'S DECLARATION

Hereby I declare, that I have written this thesis independently.

No academic degree has been applied for based on this material. All works, major viewpoints and data of the other authors used in this thesis have been referenced.

"....." 20.....

Author: Naveenraj Akkam Veetil
/signature /

Thesis is in accordance with terms and requirements

"....." 20....

Supervisor: Hadi Ashraf Raja
/signature/

Accepted for defence

"....."20... .

Chairman of theses defence commission:
/name and signature/

Non-exclusive Licence for Publication and Reproduction of Graduation Thesis¹

I, Naveenraj Akkam Veetil (name of the author) (date of birth: 05/09/1995) hereby

1. grant Tallinn University of Technology (TalTech) a non-exclusive license for my thesis Fem based modelling and analysis of eccentricity faults in induction motors.

supervised by

Dr Toomas Vaimann, Senior Researcher

Mr Hadi Ashraf Raja, PhD Student

(Supervisor's name)

1.1 reproduced for the purposes of preservation and electronic publication, incl. to be entered in the digital collection of TalTech library until expiry of the term of copyright;

1.2 published via the web of TalTech, incl. to be entered in the digital collection of TalTech library until expiry of the term of copyright.

1.3 I am aware that the author also retains the rights specified in clause 1 of this license.

2. I confirm that granting the non-exclusive license does not infringe third persons' intellectual property rights, the rights arising from the Personal Data Protection Act or rights arising from other legislation.

¹ *Non-exclusive Licence for Publication and Reproduction of Graduation Thesis is not valid during the validity period of restriction on access, except the university's right to reproduce the thesis only for preservation purposes.*

_____ *(signature)*

_____ *(date)*

Department of Electrical Power Engineering and Mechatronics

THESIS TASK

Student: Naveenraj Akkam Veetil (name, student code)

Study programme, MAHM02/12-Mechatronics (code and title)

main speciality:

Supervisor(s): Dr Toomas Vaimann, Senior Researcher

Co-supervisor: Mr Hadi Ashraf Raja, PhD Researcher

Thesis topic:

(in English) Fem based modelling and analysis of eccentricity faults in induction motors

(in Estonian) Lõplikel elementidel põhinev asünkroonmootorite ekstsentrilisuse modelleerimine ja analüüs

Thesis main objectives:

1. *In-depth study of Airgap Eccentricity faults in induction motors.*
2. *Study and implement modelling and simulation of the healthy and faulty motors*
3. *Comparative analysis of the results*

Thesis tasks and time schedule:

No	Task description	Deadline
1.	Literature review	01/02/2021
2.	Understanding the faults and diagnosing techniques.	25/02/2022
3.	Modelling of Induction motor	20/03/2022
4.	Result analysis and writing	25/04/2022

Language: English **Deadline for submission of thesis:** "18/05/2022"

Student: Naveenraj Akkam Veetil "....."2022
/signature/

Supervisor: Dr Toomas Vaiman "....."2022
/signature/

Co-supervisor: Hadi Ashraf Raja "....."2022
/signature/

Head of study programme: Prof. Anton Rassõlkin.. "....."2022
/signature/

Terms of thesis closed defence and/or restricted access conditions to be formulated on the reverse side

CONTENTS

List of Tables.....	8
PREFACE.....	9
List of abbreviations and symbols.....	10
1. INTRODUCTION.....	11
2. LITERATURE REVIEW AND BACKGROUND	13
2.1 Fault diagnosis using FEM	13
2.2 Fault diagnosis using MATLAB	17
2.3 Fault diagnosis using LabVIEW.....	18
2.4 Fault diagnosis using ANSYS	18
2.5 Conclusion of literature review	19
3. INDUCTION MOTORS	20
3.1 Design and working principle of induction motor.....	20
3.2 Types of faults in induction motors	27
4. MODELLING AND SIMULATION.....	32
4.1 Healthy motor	32
4.1.1 Healthy induction motor analysis using Ansys Maxwell 2D	33
4.2 Faulty motor.....	35
4.2.1 Faulty induction motor analysis using Ansys Maxwell 2D.....	36
4.3 Mathematical expressions for eccentricity	40
4.3.1 Frequency components of the faulty motor	40
5. RESULTS AND DISCUSSIONS	41
5.1 Transient analysis of Healthy induction motor without load.....	41
5.2 Transient analysis of Healthy induction motor with load	45
5.3 Transient analysis of Faulty induction motor without load.	49
5.4 Transient analysis of Faulty induction motor with load.....	53
5.6 Co-simulation of Ansys and Matlab	56
5.7 FFT analysis of motor in load conditions	57
6. CONCLUSION	61
SUMMARY.....	62
SUMMARY IN ESTONIAN.....	63

REFERENCES.....	64
-----------------	----

List of Figures

Figure 3.1 Stator of a three-phase induction motor.	21
Figure 3.2 Induction motor rotor types	22
Figure 3.3 Labeled diagram of induction motor	23
Figure 3.4 Six salient pole three-phase induction motor.	24
Figure 3.5 Instantaneous values of current and position of flux.....	25
Figure 3.6 Rotor stator rub caused by air gap eccentricity fault.....	29
Figure 3.7 Rotor mass unbalanced fault.	29
Figure 3.8 cross-section of induction motor a) healthy b) static and c) dynamic eccentricity.	30
Figure 4.1 RMxprt model of Healthy Induction motor.	32
Figure 4.2 Geometry design.....	33
Figure 4.3 Magnetic flux density of healthy motor.	35
Figure 4.4 Negative x-axis air gap.	36
Figure 4.5 Positive x-axis air gap.	37
Figure 4.6 Positive x-axis air gap.	37
Figure 4.7 Positive y-axis air gap.	38
Figure 4.8 Negative y-axis air gap.	39
Figure 4.9 Magnetic flux density of faulty motor.....	39
Figure 5.1 Transient analysis of the moving torque.....	41
Figure 5.2 Transient analysis of current.....	42
Figure 5.3 Transient analysis of Phase A.....	42
Figure 5.4 Transient analysis of Induced voltage.....	43
Figure 5.5 Transient analysis of flux linkages.....	43
Figure 5.6 Transient analysis of voltages.....	44
Figure 5.7 Transient analysis of power	44
Figure 5.8 Transient analysis of power	45
Figure 5.9 Transient analysis of the moving torque.....	45
Figure 5.10 Transient analysis of current.....	46

Figure 5.11 Transient analysis of Phase A.....	46
Figure 5.12 Transient analysis of induced voltages	47
Figure 5.13 Transient analysis of flux linkages.....	47
Figure 5.14 Transient analysis of voltages.....	48
Figure 5.15 Transient analysis of powers	48
Figure 5.16 Transient analysis of the moving torque.....	49
Figure 5.17 Transient analysis of current	50
Figure 5.18 Transient analysis of phase A.	50
Figure 5.19 Transient analysis of induced voltages.....	51
Figure 5.20 Transient analysis of flux linkages.	51
Figure 5.21 Transient analysis of voltages.....	52
Figure 5.22 Transient analysis of powers.	52
Figure 5.23 Transient analysis of current.....	53
Figure 5.24 Transient analysis of phase A.	54
Figure 5.25 Transient analysis of induced voltages.....	54
Figure 5.26 Transient analysis of flux linkages.	55
Figure 5.27 Transient analysis of voltages.....	55
Figure 5.28 Faulty motor with load conditions.	58
Figure 5.29 Healthy motor with load conditions.	58

List of Tables

Table 4.1 Stator dimensions.	33
Table 4.2 Rotor dimensions.....	34
Table 4.3 Operating conditions.....	34
Table 5.1 Validation of frequency component in steady state.....	59

PREFACE

The motor is used to convert electrical energy into mechanical energy. Three-phase induction motor is one of the types of electrical motor. These days, three-phase is one of the most used AC motors to produce mechanical power in worldwide industries. The commonly seen problems in induction motors are bearing faults, eccentricity faults, unbalanced stator and rotor faults and winding faults. 80 percent of the faults in Induction motors are caused by Airgap eccentricity, which makes the production of the industries difficult in certain situations. This thesis aims to identify the reason and the factors that lead to air gap eccentricity. The distance between rotor and stator is equal for a healthy motor. It could change because of particular reasons which lead to a defective motor. The different methods for diagnosing faulty motors help identify and prevent the consequences. The modeling and simulation of the induction motor were done using Ansys software. The model was constructed with the help of the RMxpert tool, which was converted into 2D and 3D models. Then the simulation was conducted for 5 minutes and collect the data. This data was used for FEM and FFT analysis. The results graphs were generated as an output of the analysis such as induced current, induced voltages, moving torque, flux linkages, electrical and mechanical properties.

List of abbreviations and symbols

FEM	- The Finite Element Method
FM	- Faulty motors
HM	- Healthy motors
FFT	- Fast Fourier Transform
SE	- Static eccentricity
DE	- Dynamic eccentricity
ME	- Mixed eccentricity
FEA	- Finite element analysis
TSFE	- Time stepping finite element
IM	- Induction Motor

1. INTRODUCTION

Induction motors are one of the most widely used machines because of their high reliability, efficiency and performance. It has a significant role in modern industries. As well as the advantages, the Induction motor has its faults, which is becoming a massive issue in big production plants and mechanical industries.

The commonly seen problems in induction motors include bearing faults, eccentricity faults, unbalanced stator and rotor faults and winding faults. Around 80% of these faults in Induction motors are caused by Airgap eccentricity, which can cause issues for the production line in the industry [1]. Mainly the defects occur due to the oval structural design of the motor, the assembling errors, over speed, and overload of the motor.

Also, in thermal power plants, it is pretty challenging to solve the motor issues in a short time and take a considerate period to identify and resolve such issues. Similarly, in large-scale industries, the work has been shut down for 3-4 months for the maintenance of the faulty and healthy machines, which is a very long and time-consuming process. During the previous decades, it was difficult to detect faults in the motor at an earlier stage and were usually found during a shutdown or maintenance. These shutdowns create financial losses for the company, so it is necessary to diagnose the faults quickly and precisely.

Most commonly occurring faults in an induction motor are either caused by an electrical, environmental or mechanical issue. Some of these faults are easy to detect, whereas it is hard to identify and pinpoint the source of the issue in some cases. One such case can be the displacement of the rotor inside the induction motor, which can result in more significant losses if not detected at an earlier stage. This work studies the eccentricity faults, how to work on FEM transient analysis, compare healthy and faulty motor frequency components and suggest a solution for such issues.

Objectives

The aim of this thesis is to identify and filter out the frequency components that are present inside a faulty induction motor due to eccentricity faults. By running simulations of problems and identifying the prominent components, we can look into the following things.

- What is the effect of displacement of the rotor from its position?
- What are the Eccentricity faults in Induction motors?
- How are they produced?

- What are the characteristics of Voltage and Current signature/frequency components once the rotor is displaced?
- Does the distance of displacement affect the frequency components in any way?
- Can this displacement be detected using Finite Element Analysis?
- Is it possible to identify specific frequency components to detect such faults?

2. LITERATURE REVIEW AND BACKGROUND

2.1 Fault diagnosis using FEM

Mohamed Moustafa and Mahmoud Sedky had worked on the eccentricity faults of the motor with the help of FEM. The main faults that they tried to rectify are the static, dynamic and mixed eccentricity. The condition provided in the study is that the model is analyzed both in load and no-load. For the model, the Line-start permanent magnet synchronous motors were used. Since the experiment was performed in real-time, it was challenging to find a way to solve the non-linearity of the motor using the simulation technique. Also, the author concludes the work by finalizing the result, which the load test has a damping effect on the motor and helps decrease the fault with no-load [2].

In 2014, Zaabi W et al. researched fault analysis of induction machines using the Finite Element Method (FEM). This paper introduced an efficient induction motor analysis technique based on finite element analysis(FEA). The FEM analysis provides much more knowledge than the classical theoretical models on the phenomenon characterizing the operation of electrical machines. To detect the faults, electromagnetic flux, torque and stator current of FFT analysis of motor is used [3].

In 2020, Liang X. et al. researched induction motors fault diagnosis using finite element methods. Three research streams are used in this paper using the FEM for the diagnosis of induction motor fault is reviewed in the literature:

- 1) Approach to FEM-based fault diagnosis
- 2) FEM and signal approach based on processing
- 3) FEM, machine learning, and other advanced technique-based approaches

As a powerful tool for electric machine analysis, the FEM model can provide accurate modeling for various faulty conditions of the machine. It offers insight and needed signals for further analysis using signal processing in machine learning. In this study, they have used 2 approaches, FEM combined with signal processing and FEM combined with machine learning and other advanced techniques. FEM combined with signal processing is the most used method in their studies. Machine learning is widely used in various fields, its application in induction motor fault diagnosis is increasing nowadays [4].

In 2018, Galina M and Saad, Khalid Imtiaz worked on rotor faults and eccentricity of Induction Motors. The research is mainly based on internal flux measurement. This

paper describes a comprehensive model of a stable induction motor's air gap flux density and a motor with rotor bar and eccentricity faults. A new fault detection technique has been proposed based on this analysis and sophisticated instrumentation by a series of Hall Effect Flux Sensors mounted in the motor air gap. This paper proposes a practical model for combining stator and rotor flux densities in the motor air gap. They measured the primary flux density concerning both time and space with the help of miniature Hall Effect Flux Sensors (HEFS) array installed around the circumference of the stator inside the motor air gap.

Based on this instrumentation, an advanced technique is proposed to detect and localize the rotor bar faults and mixed eccentricity. It also demonstrates how the proposed technique effectively discriminates between the different fault conditions. The core content of this paper is a well-defined model of the induction motor, including both stator and rotor components for a healthy and a faulty motor in addition to air gap flux density with respect to time and space dimensions. In summary, the rotor bar fault, static and dynamic eccentricity have been successfully detected in isolation during the presence of each other and their magnitudes and locations were determined correctly. Therefore, the fault diagnosis principles proposed in this paper have been successfully validated. [5]

In 2017 Ahcene et al conducted a study on the dynamic eccentricity of induction motors by using FEM. The simulated results are close to the experimental ones in the case of the dynamic eccentric machine. However, all newly constructed machines are said to possess small dynamic and static eccentricities due to manufacturing conditions. In an induction motor, more significant load oscillations may lead to an unbalanced magnetic pull on the rotor. This may occur for an extended period, and resulting in an increase in eccentricity level in the induction motor. The proposed FE model based on the real parameters of the tested machine describes the physical behavior of the machine under fault conditions and the results are successfully closed to the experimental case [6].

In large-scale industries, eccentricity faults are a big problem. Due to eccentricity fault, the production line had to stop for maintenance several times in a year. Since the motor can be unavailable, it is not easy to diagnose the fault. Faiz and Ebrahimi developed a time-stepping finite-element approach (FEM). It detects mixed eccentricity without direct access to the motor. This methodology overcomes the challenge of adapting transient actions to FEMs. It simulates the line current spectrum of a production line motor and compares it to an established stable motor spectrum to detect eccentricity. [7].

Polat et al. worked on the method to analyze the 3 types of eccentricity faults using the FEM method in 2015. They modeled the squirrel gage induction motor by adding particular materials and specific boundary conditions, meshing, and arranging the FEM for the derived equations. They Used Comsol software for modeling and FEM analysis. Static, dynamic and mixed eccentricity faults have been explained enormously for better clarification of the faults. For this research, they have designed a working model of a three-phase induction motor and simulated it using comsol software. Results and test results were examined for each case. Finalized that the faults can be informed with vibration analysis. [8].

In 2015, Jawad Faiz and Vahid Ghorbanian studied broken rotor bars in industrial induction motors. A new analytical and experimental aspect of fault are proposed using the motor variables' time and frequency domain variations such as current, voltage, electromagnetic torque, and speed.

To achieve a precise fault diagnosis, properly select processed signals, processing tool and output index. The progressive steps of the fault diagnosis methods could be divided as follows

- (1) Select a proper domain (time, frequency, time-frequency) to analyze the signal.
- (2) Selecting an appropriate signal.
- (3) Applying an appropriate processor
- (4) Extracting a merely rotor broken-bar related index enables the experts to precisely diagnose the fault.

Three different analysis procedures based on time, frequency and time-frequency were presented in this paper through the progressive development of the concepts of the rotor broken bar fault [9]

Induction Motor under Eccentricity Fault based on Finite Element Analysis was researched by Jalila et al. in 2019. In the example of a three-phase induction motor, the paper focused on the identification of static, dynamic, and combined eccentricities. They concluded that the mixed eccentricity fault is the most significant anomaly on the IM stator current. It is the most significant flow with more than 50% distortion. As a result, the IM failure is amplified [10].

In 2015, Subramanian J et al. approached a different type of analyzing method for detecting the eccentricity faults in an induction motor. The model has been developed in maxwell software to examine the difference of experimental and simulated results. A motor was developed with two cases. 20 percent and 40 percent dynamic eccentricity.

The defined eccentricity model had undergone four different load test to get variant results. The two detection schemes were researched by using the FEM model. The parameters has been verified are frequency and voltage [11].

In 2019, Hossein et al. researched the topic of time-stepping finite element(TSFE) analysis of IM under static and dynamic eccentricity faults. A different approach called "virtual blocked rotor technique" was used to reduce the calculation time. In this method, the calculations can only be done at one instant, compared to the time-stepping Finite element method of the motor with the required ac cycles. Utilizing TSFE and VBR method, the torque is obtained from the simulation. Slip and operating points were added to the frequency domain solver to modify the material conductivity and resistance of the rotor. The frequency spectrum of the stator is also analyzed in this paper [12].

In 2017, Prasob K et al. researched a journal about Turn Short Circuit Fault Analysis of PWM Inverter Fed Three-Phase Induction Motor Using Finite Element Method. This paper deals with the Pulse Width Modulated (PWM) three-phase IM Inter-turn short circuit fault analysis using the FEM. In this research, FEM is used for studying the distribution of magnetic field and radial air gap flux density of IM. It is evident from the findings that flux lines are distributed symmetrically in the safe motor, while a major distortion in flux lines below the defective state of 25 percent and 50 percent inter-turn. [13].

In 2018, Vinothraj, C et al. researched bearing fault analysis in IM drives using FEM. This study analyzes the FE approach to analyze an induction engine's electromagnetic field with a bearing loss supplied by mains and a three-phase voltage source PMW inverter in the open belt. Parameters of electric-magnetic fields such as distribution of flux lines, flux density, and gap flux density in radial air were studied. The presence of bearing faults can be found by detecting Fast Fourier transform (FFT) analysis of induction machines' radial air gap flux density. The width of the air gap increases in the main component, which leads to an increase in the fault intensity [14].

In 2019, A. Sapena-Bano et al. published a paper on an induction machine model with finite element accuracy for condition monitoring running in real-time using hardware in the loop system. An accurate model of faulty and non-faulty induction motors was developed for the experiment by using the FEA. For the model, symmetric and anti-symmetric conditions were added to the model's boundary conditions. The circuit model was performed in Matlab software. A comparison between the real-time model and simulated model for the work was made to test the model; the signals should be generated from the embedded systems for diagnosing the faults. Static current spectrum was analyzed for both the real-time model and the proposed model. [15].

In 2019, Adel Ghoggal and Amel Hadri Hamida presented the topic of Transient and steady-state modeling of healthy and eccentric induction motors considering the main and third harmonic saturation factors. The work holds regular and irregular airgap detection. Simulations were conducted in a healthy state and airgap faulty state. The testing was done by varying the voltage levels. Simulations are done by 2 different models for the estimation of EMF. The second simulation is by two different load conditions. Experimental and simulated results in two models had given similar results. The calculations of the integrals happen to the performance of inductance in mathematical arrangements. The analysis findings are mentioned as the airgap technique was successful, for highly high saturation fault severity is noted. [16].

2.2 Fault diagnosis using MATLAB

In 2015, Sathish R. et al. researched the topic "Analysing and Detection of Rotor Faults in Squirrel Cage Induction Motor Drives Using MATLAB". Rotor speed and current frequency spectrum were closely analyzed in this method. The simulated induction motor model undergoes FFT analysis, and the output of the analysis gives the spectrum graphs of stator current. The possible outputs from the analysis can be either the motor running in a healthy state or warning state or a faulty state. The state of the motor is sent to the supervision station through GSM so that the operator can take necessary action. The proposed system owes to detect the rotor faults in squirrel induction cage motors at a very early stage and prevents any hassles in the operation of the motor. The broken rotor bars in the squirrel cage induction motor were early found using the stator current analysis alone. The necessity of various sensors like torque, temperature, and vibration sensors was eliminated [17].

In 2016, Ruchira Patole and Monika Bhagwat researched a paper about detecting rotor and eccentricity faults in three-phase IM using sound analysis. This paper deals with the sound analysis of three-phase IM. The sound for the test motor was analyzed to work on the gain of the motor. Important variations in the noise spectrum between stable motors and engines with distinct faults are observed. The faults studied are split rotor bar faults and eccentricity faults. The spectral noise study of the wavelets produces a method for the identification of faults. The sound frequency on an excellent engine is 30-33 dB and for a rotor, a fault engine is 45-50 dB. The estimated sound frequency for an eccentricity fault engine is 55-60 dB. The waveforms are equivalent to the reference noise continuum from the stable generator. [18].

2.3 Fault diagnosis using LabVIEW

In 2015, Ramprasath E and Manojkumar P researched modeling and analysis of IM using LabVIEW. It helped to simulate the motor to evaluate the output. The model was designed with the help of mathematical expressions and values. The simulation was done in labview for the torque vs speed and a load test model. For the torque vs speed simulation, the model was constructed using GUI. While in the case of load test simulation, the efficiency has a greater influence on greater load. When the load given is more, the efficiency is more. The testing and analysis in a real-time motor require more time and cost [19].

In 2014, Gunabalan R. et al. researched the topic of Simulation of Inverter Fed Induction Motor Drive with LabVIEW. The selection of LabVIEW software is because of its solid graphical interface, the flexibility of its programming language, and built-in tools designed specifically for test, measurement, and control. LabVIEW is generally used in most applications for data acquisition, test and control. This paper modulates the inverter and induction motor using LabVIEW toolkits. The labview work procedures include different state variables used for integration, and the calculation of speed and torque is calculated from stator voltages and currents [20].

2.4 Fault diagnosis using ANSYS

In 2016, Praveen Kumar N. Isha T. B. [21] the electromagnetic features of PWM inverter fed IM are investigated using the FEM model for healthy and single broken bar faults in this research. A study of the magnetic field distribution of the healthy and faulty motor models is conducted because a single broken bar fault is difficult to detect. The analysis reveals deformation in the axis of magnetic poles. It causes saturation in the rotor and stator teeth near the broken bar, resulting in torque and speed oscillations. The FFT Spectrum of healthy and faulty IM has been compared and the radial airgap flux density to the air gap distance. The simulation results clearly show that magnetic noise has been introduced into the FFT spectrum of the broken bar motor.

This paper gives two different versions of a simulation platform for defect detection in electric drives. The drive of an inverter-fed three-phase induction motor was modeled using two alternative methodologies. The IM was modeled by using Simulink software and Ansys maxwell. In Maxwell, the model is initially made in the RMxpert tool, later the model is changed to maxwell 2D. Also, the Maxwell model has been simulated for a

given time period in load conditions to get varied results. The output of both the software models has been examined. [22].

In 2014, Z.Ferkova researched the work on the design and the simulation of 2 phase induction motors. The work was about the comparative study of designed models. The steps taken are that the model is introduced in Ansys maxwell software, in 2D and 3D. The proposed design is simulated in Maxwell and the results are compared in Matlab. The data collected is used for Simulink and analyzed the frequency, voltage and torque. The differences between the healthy and faulty models have been well analyzed and explained in work very precisely. But the lack of explanation in getting a proper result and accuracy is a disadvantage in work [23].

2.5 Conclusion of literature review

This chapter reviews the IM parameter, estimation, and fault diagnosis with variable methods.

- The study of the literature survey provides in-depth information about the IM
- FEM needed a large amount of data as input for the mesh used in nodal connectivity and other parameters depending on the problem.
- The execution time required for FEM is quite large.
- Output results will vary considerably.

The methods of these studies require further improvements:

1. Improvements to the software used to model a healthy IM.
2. Accuracy in taking data collection for the comparison with faulty IM
3. Specific and scientific evaluation methods

Scope of work

- An overview of induction motor and fault diagnostics.
- In-depth study of Airgap Eccentricity faults in an induction motor.
- Study and implement modeling and simulation of healthy and fault motor.
- Study of FEM, FFT analysis for induction motor.
- A Comparative analysis of frequency components at different states.
- Identification of the frequency components and validating them.

3. INDUCTION MOTORS

In industries, commercial areas and at the domestic level, Induction motors are widely used nowadays. The machine is simple, rugged, low in price and easy to maintain. Normally, three-phase induction motors are used in industries on a large scale, while single-phase induction motors are used on a smaller scale. For example, in water pumps, refrigerators, air conditioners, fans, etc. In these machines, voltage and current (which produces rotor magnetic field) are induced in the rotor through the stator's magnetic field, hence the name "Induction motors". Three-phase induction motors are self-starting and single-phase induction motors are started by some external means like capacitor etc.

Induction motors are also called asynchronous motors because they never run at synchronous speed (speed of three-phase stator's magnetic field). An induction motor cannot run at synchronous speed because the electromagnetic induction will stop at synchronous speed, and the motor will also stop. Hence, the term "Slip" is defined in induction motors. Slip is the value of rpm that an induction lags the stator's magnetic field while running. The assembly of the induction motor and induction generator is almost the same. So, they can be used alternatively. However, induction generators are less common compared to induction motors.

3.1 Design and working principle of induction motor

An induction motor consists of two main parts.

3.1.1 Stator

The stationary part of the motor consists of a steel frame that supports a hollow cylindrical core made up of laminations. There are several slots available depending on the size and specification of the motor. These slots hold stator winding. The stator in a three-phase induction motor has three windings. These windings are 120° apart to produce a revolving magnetic field. This revolving magnetic field induces a voltage in rotor windings. While stator of a single-phase induction motor has two windings. One winding is called starting winding and the other is running winding. Starting winding only helps to start the motor. The stator of three-phase induction motor is shown in figure 3.1.



Figure 3.1 Stator of a three-phase induction motor.

3.1.2 Rotor

The rotating part of the induction motor is called a rotor. The induction motor's rotor produces a magnetic field using electromagnetic induction phenomena. It is composed of punched laminations. These laminations are punched carefully to attain space for rotor windings. Rotor winding of induction motor has two types.

Wound rotor winding is a conventional winding method by using insulated copper or any metallic wire. Three-phase winding is done if the motor is a three-phase induction motor. The three-phase rotor winding is usually Y-connected. It's also called a slip ring induction motor. Slip rings are provided to produce high starting torque by adding external resistance to the rotor circuit. Ends of three-phase rotor winding run on slip rings can be used either to examine rotor current or add extra resistance if needed.

Squirrel Cage winding is also used in a three-phase induction motor. The rotor consists of a series of conducting bars short-circuited at their ends via shorting rings. This conducting bar design resembles the exercise wheel that the squirrel runs on. Hence the name "Squirrel cage". The stator and rotor have a minimal air gap of order 0.4mm to 4mm.

These two types of motor windings give rise to two induction motors. One is a squirrel cage induction motor and the other is a wound rotor induction motor. Two types of rotor designs are shown in figure 3.2.

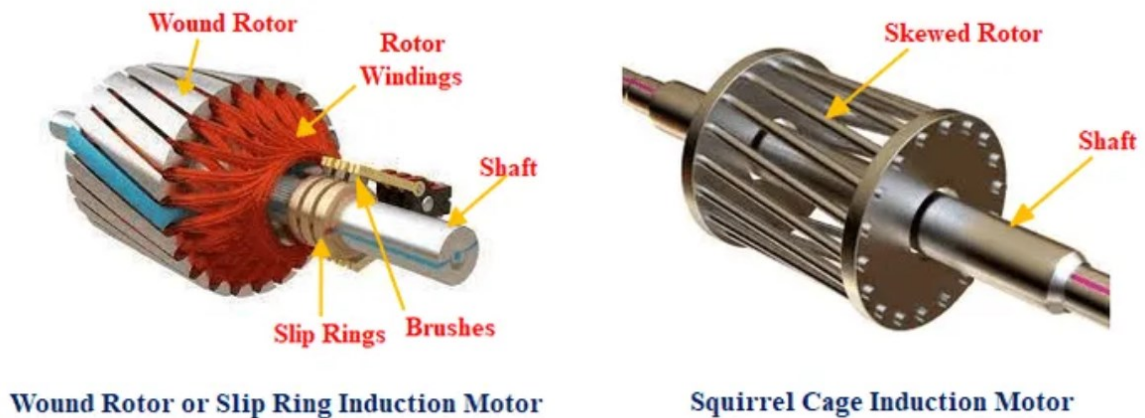


Figure 3.2 Induction motor rotor types [24]

Other parts of the induction motor are given as,

- **Fan cover** to protect the fan from the external environment.
- **Cooling fan** is used to cool down the stator and rotor winding while running to prevent excessive heating.
- **End bell** holds a bearing to separate the moving shaft from the stationary stator casing.
- **Wiring box** houses terminals to provide electric supply to stator winding of induction motor.
- **Lifting eye** is used to lift the motor utilizing a chain or rope.
- **Cast iron casing** houses the stator core, stator windings, and rotor. In general, it houses the main assembly of the induction motor.
- **Name plate** has the specification of the induction motor.
- **Stator coils** have AC which produces a magnetic field to operate.
- **Squirrel cage rotor** in this case, is revolving part of the motor discussed earlier. It can be a wound type rotor.
- **Ball bearing** is used to separate the shaft from cast iron casing.
- **Bearing seal** protects lubricants from leaking out

A labeled diagram of the induction motor is shown in Figure 4 (Ahmed Faizan Sheikh 2018).

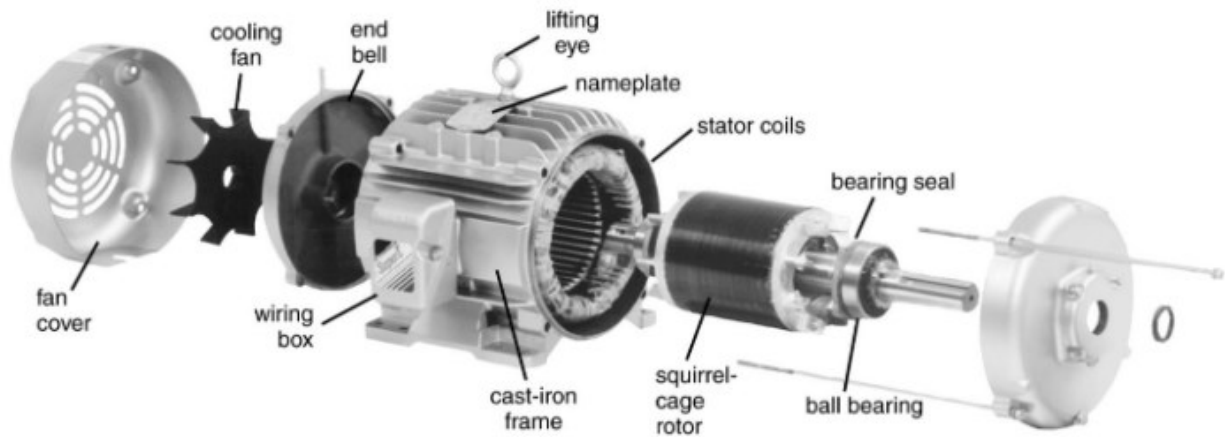


Figure 3.3 Labeled diagram of induction motor [25]

3.1.3 Working principle of induction motor

When a three-phase AC voltage is applied to the stator winding, then current flows in stator windings to produce a revolving magnetic field. The stator has three winding that are displaced by 120° from each other. So, the current flowing in these windings is also displaced by 120°. The rotating magnetic field revolves at a synchronous speed that is measured by the formula given below,

$$\text{Synchronous speed} = \frac{120 * f_e}{P}$$

Where, 'fe' is the electrical frequency of the source. It is typically 50Hz or 60Hz. And 'P' is the number of poles.

The rotating flux crosses the air gap to link with rotor windings. The rotating flux is variable as it is produced through AC supply and it's revolving as well. Air gap acts as a high reluctance path to magnetic flux, this will be discussed later. When rotating flux cuts the rotor windings, a voltage is induced in rotor windings according to "Faraday law of electromagnetic induction". As the rotor circuit is closed circuit both in the case of wound rotor and squirrel cage, a current starts flowing in the rotor circuit, which produces a magnetic field. Both magnetic fields interact with each other to produce a force on rotor. Rotor starts running in the direction of the rotating magnetic field.

To understand the revolving magnetic field, let's consider a 6 salient pole three phase induction motor as shown in figure 3.4.

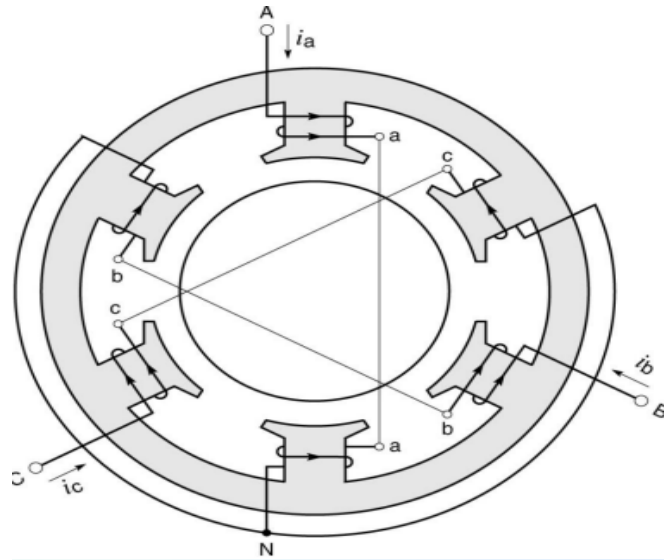


Figure 3.4 Six salient pole three-phase induction motor.

Each pole has a coil of 5 turns. Opposite coils are connected in series to produce one winding. Each winding produces a magneto motive force that acts in the same direction. Windings are Y-connected, and three ends are provided with a balanced supply. We have AN, BN, and CN phases that are 120° apart. The current in these windings will flow in such a way that three currents are 120° out of phase from each other. So, magnetic field produced will be rotating. The direction of rotation depends upon phase sequence. If direction of rotation is clockwise for 'abc or positive sequence', then it will be counterclockwise for 'acb or negative sequence'. So, the phase sequence should be correct to rotate induction motor in right direction. The value of current will be different at different instants with respect to time. The instantaneous values of currents and corresponding position of flux for one complete cycle is given in figure 3.5.

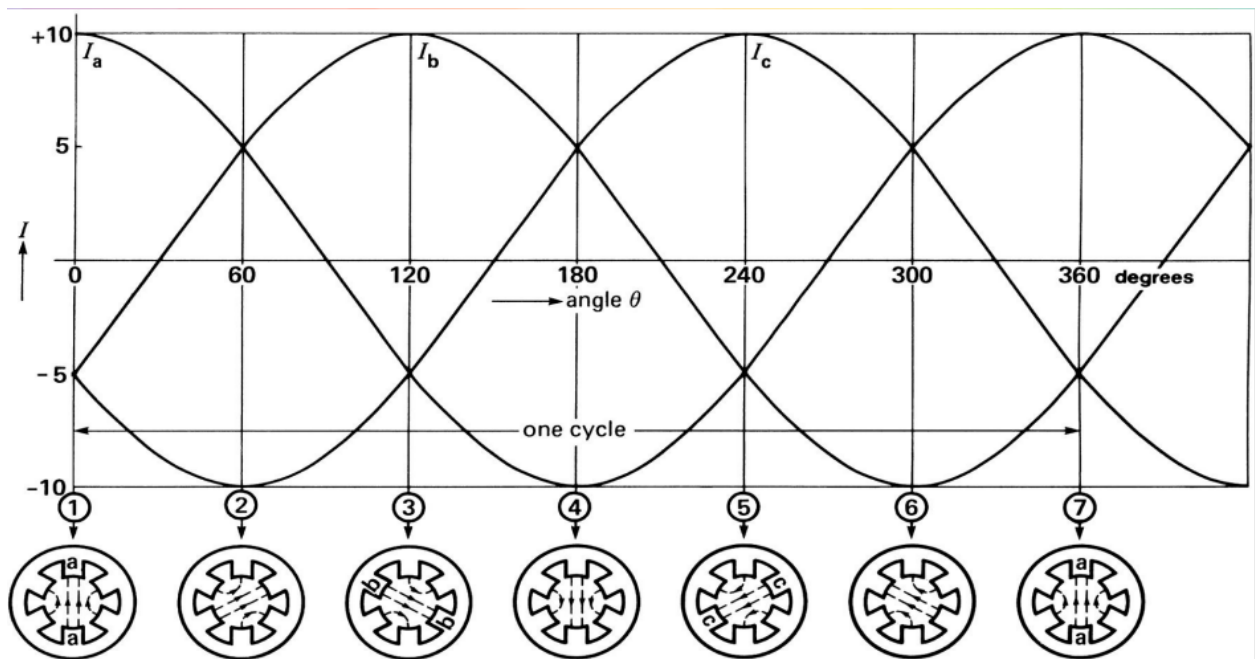


Figure 3.5 Instantaneous values of current and position of flux.

Induction motors used in real-world have many turns which produce a very strong rotating magnetic field. This field exerts a torque on rotor which rotates it. Induction motors always lag the synchronous speed. The term "Slip" comes into play. Slip is the value of rpm that rotor of induction motor lags the speed of stator magnetic field. % Slip can also be found by using the formula given below,

$$\% \text{ Slip} = \frac{(\text{Synchronous speed} - \text{Actual speed})}{\text{Synchronous speed}} * 100$$

It ranges from '0' to '1'. The slip of the induction motor is maximum when the rotor is standstill or blocked. Slip will be zero at synchronous speed.

Three-phase induction motors can be self-started. However, to facilitate starting number of methods are used. They are different for two types of induction motors.

Starting methods of squirrel cage induction motor:

1. Direct online starting

2. Stator resistance starting
3. Autotransformer starting
4. Star delta starting

Starting methods of wound rotor induction motor:

1. Direct on-line starting
 2. Stator resistance starting
 3. Auto transformer starting
 4. Rotor resistance starting
- Advantages and Disadvantages of Induction Motor:

Advantages:

- Construction of an induction motor is very simple as its rotor doesn't need any DC supply as in synchronous machines or any brushes like in DC machines. Its construction is robust and rugged. So, it can operate in any environment.
- It's very cheap as compared to other electrical motors due to the absence of some components that are present in other motors.
- Induction motors are self-starting, unlike other three-phase machines.
- Absence of brushes prevents it from sparking. It allows us to operate induction machines in dangerous conditions as well.
- They have controllable starting torque and good load capacity.
- Induction motors have good efficiency, especially near full load.
- Only an AC source is used to operate the induction machine, unlike a synchronous machine which needs DC excitation.

Disadvantages:

- Power factors is very low at light loading.
- Self-starting technique for induction motors.
- Speed control of induction motor is very difficult
- Decreased efficiency at light loading as copper loss is higher due to large current.
- Induction motors have poor starting torque, it cannot be used in applications where starting torque is high.
- Starting current is large, it causes a massive glitch in voltage.

3.2 Types of faults in induction motors

There are multiple types of faults in induction motors, a most seen fault is explained below:

3.2.1 Electrical faults

Electrical faults are divided into seven types of faults. Their explanation is given below.

Overload fault occurs when the induction motor is loaded beyond its capacity. Motor windings can heat up and may burn. The motor also starts to vibrate. It can be avoided by loading a motor properly.

Earth fault occurs when a phase conductor of motor winding gets short-circuited to motor casing and current starts to leak to earth. It can cause a large current and it also increases the risk of electric shock. It can be avoided by using a residual current device.

Inter Turn short circuit fault occurs when the insulation of winding gets damaged, and turns are short-circuited. it excessively reduces the resistance, which can cause a large current, and the motor may burn immediately. It can be avoided by using good-quality winding wire.

Single phasing fault occurs when one of the three phases cuts off. It's only found in three-phase induction motors. It causes excessive heating of the induction motor.

Reverse phase sequencing fault causes the direction of the motor to be changed. It can change from clockwise to counterclockwise and vice versa. It occurs due to changes in phase sequence. This phenomenon is explained earlier.

Under or Overvoltage fault occurs when supply voltage changes out of its limits.

Crawling fault occurs when a motor is accelerated in the direction of the rotating magnetic field, but it is running at 1/7th of its synchronous speed. This specific phenomenon is called crawling.

3.2.2 Mechanical faults

Mechanical faults are of three types.

Broken rotor bar fault occurs when one or more bars of the squirrel cage induction motor are broken. It's mainly due to a manufacturer defect. Non-uniform metallurgical stress can cause this.

Rotor mass unbalance fault occurs when the air gap between the outer rotor and the inner of the stator is not the same. The situation is called eccentricity. In this situation, a rotor fault occurs which is called an unbalanced rotor fault.

Bearing fault occurs when one of two or both bearings get physically damaged due to lack of lubrication or any other reason than the motor gets stuck or jammed.

Environmental faults occur when induction motors are not installed properly. For example, if the motor is vibrating. Temperature and moisture in the atmosphere can also affect the performance of the induction motor.

Air gap Eccentricity Fault, Induction motors are designed in such a way that the rotor rotates coaxially with the stator. The Axis of rotation of the rotor is the same as the axis of rotation of the stator's magnetic field. In this condition, the air gap between the stator and rotor remains the same. If the air gap between the rotor and stator gets unbalanced due to any reason, then an air gap eccentricity fault occurs. Now the rotor does not rotate coaxially with the stator.

Air gap eccentricity is a type of mechanical fault. This fault can cause severe damage to the motor, which sometimes cannot be reversed. It leads to an unequal air gap between the stator and rotor of the induction motor, which badly affects the precision and accuracy of the induction motor. It can use rub between the stator and rotor, which will severely damage the whole induction motor. The rotor will have scratches that will damage the conducting bars of the rotor in the case of the squirrel cage induction motor. It can be short-circuiting of conducting bars. A rub between stator and rotor due to air gap eccentricity fault is shown in figure 3.6.

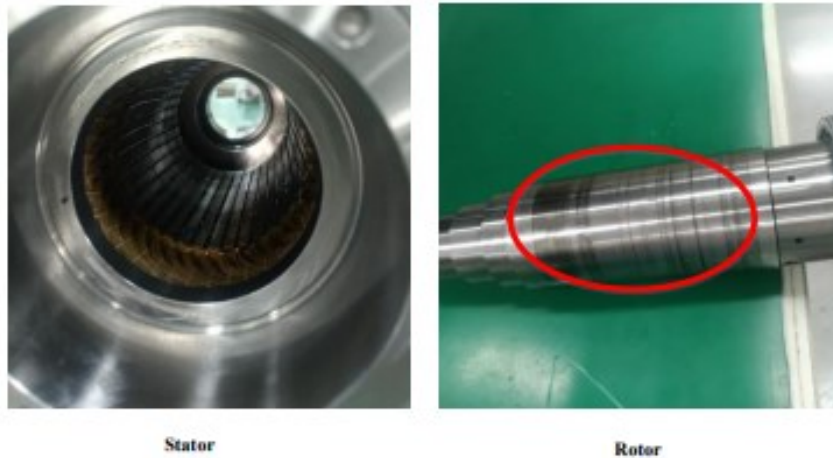


Figure 3.6 Rotor stator rub caused by air gap eccentricity fault [26].

Air gap eccentricity causes the rotor to unbalance fault, as shown in figure 3.7.

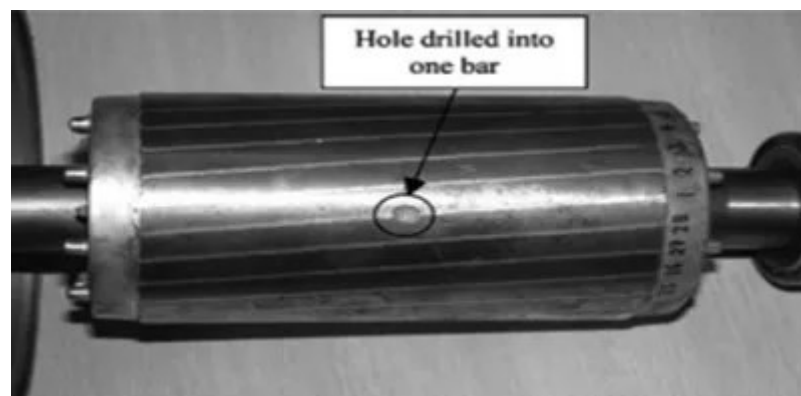


Figure 3.7 Rotor mass unbalanced fault [27].

There are three types of air gap eccentricity fault.

- Static eccentricity
- Dynamic eccentricity
- Mixed eccentricity

Static eccentricity is the condition in which the rotor rotates around its axis, but its rotational center gets displaced from the center of the stator. The area of minimum air gap will be stationary in this case.

Dynamic eccentricity is the eccentricity in which the rotor is displaced from the stator center. The geometrical center of the rotor is different from the stator's geometrical center. However, both will be the same in normal conditions. The area of a minimum gap will not be fixed now.

Mixed eccentricity is the combination of both. Mixed eccentricity is more common in induction motors. In this case, both the centers of the stator and rotor are different, and the rotational axis is also displaced.

Air gap eccentricity can be detected by continuously examining magnetic flux or by monitoring vibrations of the rotor. The current signature analysis technique is also used to detect eccentricity.

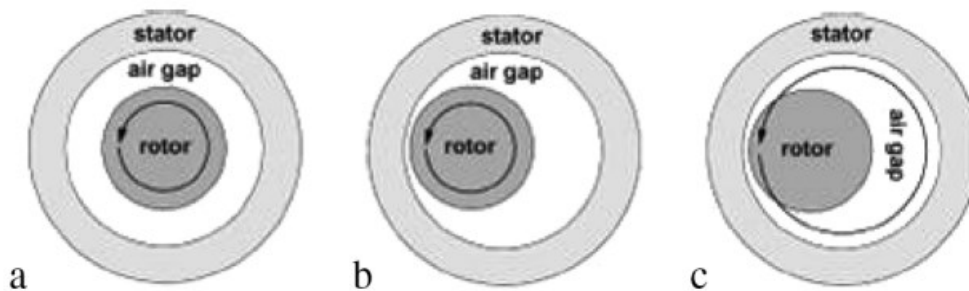


Figure 3.8 cross-section of induction motor a) healthy b) static and c) dynamic eccentricity [7].

Airgap length(LG)

There are certain factors that affect the airgap length in an induction motor. The following factors are as

1) Power factor- The larger airgap faults in the induction motor pass through the flux and causes the increasing magnetizing current that lowers the power factors. The required mmf for the air gap will be much greater than the magnetic circuit in small flux densities.

2) Overload capacity- The larger airgap length passes larger flux through the motor and the fewer turns are required for emf induction, which increases overload capacity. If the air gap is large the zig-zag leakage flux will be reduced immensely.

$$\text{Overload capacity} = \text{maximum output/ rated output}$$

3) Pulsation losses and noise- The zig-zag leakage flux vary inversely to the airgap length so to reduce the number of pulsation losses and noise, the more tendency to have a larger air gap. Also leads to the variation of reluctance due to slotting being small.

4) Unbalanced magnetic pull- If the air gap length is so small, the deflection of the rotor would eventually result in a large irregular gap. This is responsible for the production of a larger unbalanced magnetic pull. Also, if the air gap is large, a smaller deflection could not be able to make a noticeable unbalanced magnetic pull.

4. MODELLING AND SIMULATION

In this work, I had divided in to different stages. The modeling of healthy and faulty induction motor was the initial part I had done. This method was performed with the help of brilliant software, which is Ansys Maxwell. The software helped design the 3 phase Induction motor according to the defined conditions. So I modeled the 2D design of a healthy induction motor, initially with the help of Rmxprt tool. I had completed the model outline. Then the defined model structure is changed in 2D model in Ansys electronic suite by providing the parameters and values. After the process each model had done simulation for 5 minutes for getting accurate results. We run the Healthy motor and Faulty motor in 2 different conditions.

4.1 Healthy motor

The implementation of a healthy motor was done as per the methods already explained. The Rmxprt model was initially completed in this part.

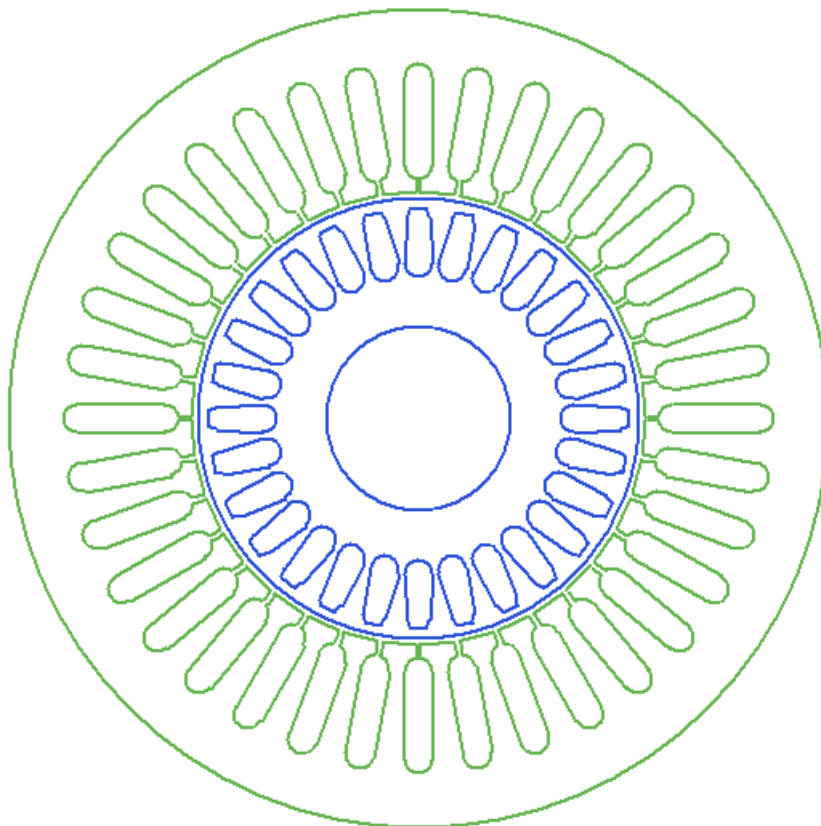


Figure 4.1 Rmxprt model of Healthy Induction motor.

4.1.1 Healthy induction motor analysis using Ansys Maxwell 2D

In order to analyze the induction motor, Ansys Maxwell 2D transient solution was used to set up a 2D model of a complete induction motor, Fig 11 shows the geometry design of the healthy induction motor.

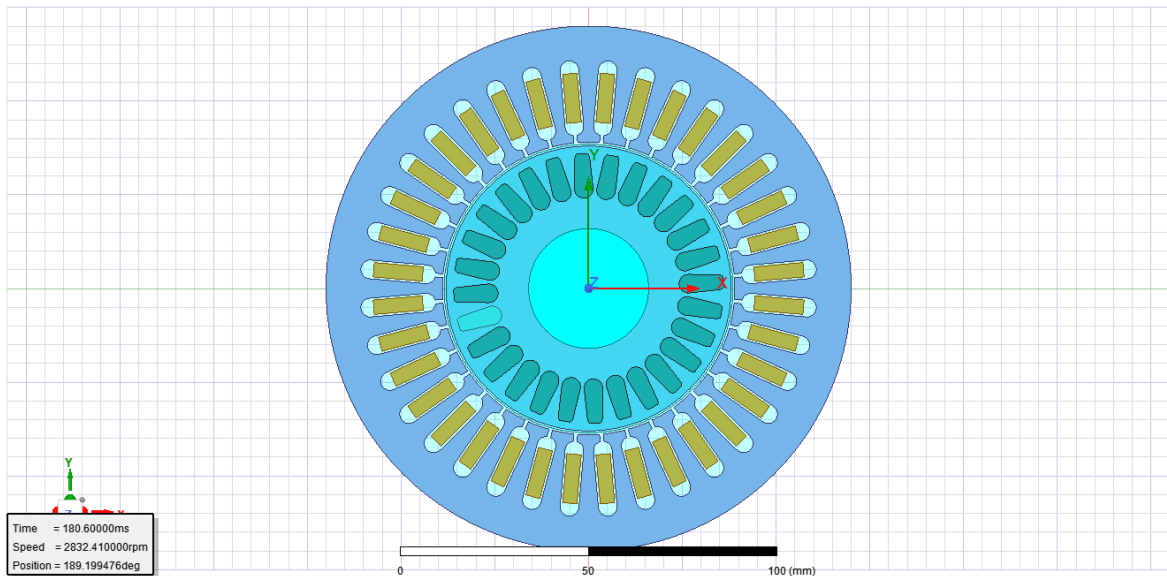


Figure 4.2 Geometry design.

The geometry in figure 4.10 was created using RMxpert, by going in the analysis section, create Maxwell design, type "Maxwell 2D design" was selected. It is an induction motor having 36 stator slots and 28 rotor slots, the design parameters for the stator and rotor of healthy induction motor are shown in Table 4.1 and Table 4.2 simultaneously.

Table 4.1 Stator dimensions.

Stator dimensions	Value	Unit
Outer Diameter	140	mm
Inner Diameter	78	mm
Length	250	mm
Stacking Factor	0.95	
Steel Type	D21_50	
Number of Slots	36	

Table 4.2 Rotor dimensions.

Rotor dimensions	Value	Unit
Outer Diameter	76	mm
Inner Diameter	32	mm
Length	250	mm
Stacking Factor	0.95	
Steel Type	D21_50	
Number of Slots	28	

Table 4.3 shows the rated output power, voltage, speed, and operating temperature. By rated we mean the conditions at which the motor designed has to run continuously.

Table 4.3 Operating conditions.

Operating conditions	Value	Unit
Rated Output Power	1100	W
Rated Voltage	380	V
Rated Speed	1500	rpm
Operating Temperature	75	cel

To introduce a motion in Ansys Maxwell transient simulation, we need to declare vacuum bands and assign the motion to the band enclosing the rotor and air gap of the motor. Three vacuum regions are introduced in the simulation named as:

- Inner region
- Outer region
- Band

The inner region is the vacuum band that encloses the rotor. The outer region covers the complete 2D motor including the rotor, air gap and stator. Lastly, the band encloses the rotor and air gap, excluding the stator.

For introducing a motion in the band, we go to model, motion setup, select motion type "rotation", moving vector in "Global Z" direction and finally, in a mechanical tab, uncheck "Consider Mechanical Transient" and put the value of angular velocity "2832.41 rpm".

Two surface approximation meshes named SurfApprox_Bar and SurfApprox_Main have been applied, SurfApprox_Bar mesh was applied on rotor slots while SurfApprox_Main mesh was applied on complete induction motor excluding the rotor slots. Figure 4.3 shows the magnetic flux density distribution in rotor and stator of the induction motor.

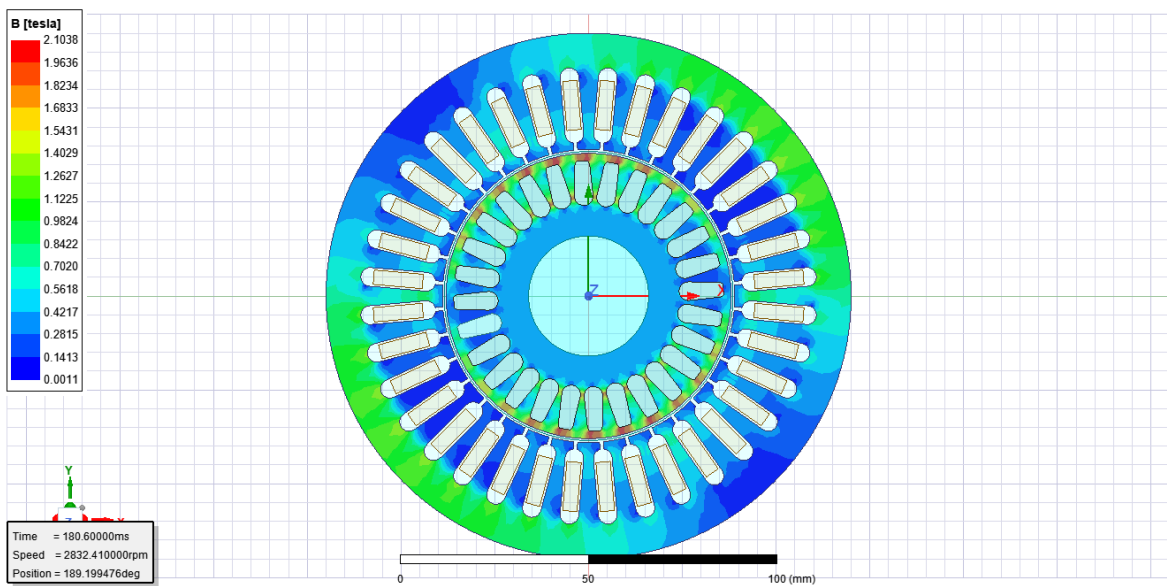


Figure 4.3 Magnetic flux density of healthy motor.

The major color in the magnetic flux density distribution is green having value 1.26 Tesla, this lies below the saturation of material, red color indicates saturation of material.

4.2 Faulty motor

The modelling and simulation of Faulty motor is divided into 2 conditions for a better clarification. The air gap values given for the motor are different in both cases to analyse the difference in results and notice the changes more precisely and accurately. The given time for the simulation of both the cases is approximately 5 minutes to check the running and the non-linearities in the airgap. Also, the results should be closely examined for clarification and further work.

4.2.1 Faulty induction motor analysis using Ansys Maxwell 2D

1st case (rotor displaced by 0.2 mm):

Non uniform air gap of 0.8mm on the negative x-axis and 1.2mm on the positive x-axis, was introduced in the Ansys Maxwell 2D model of the healthy induction motor as shown in figure 4.4 and 4.5 respectively.

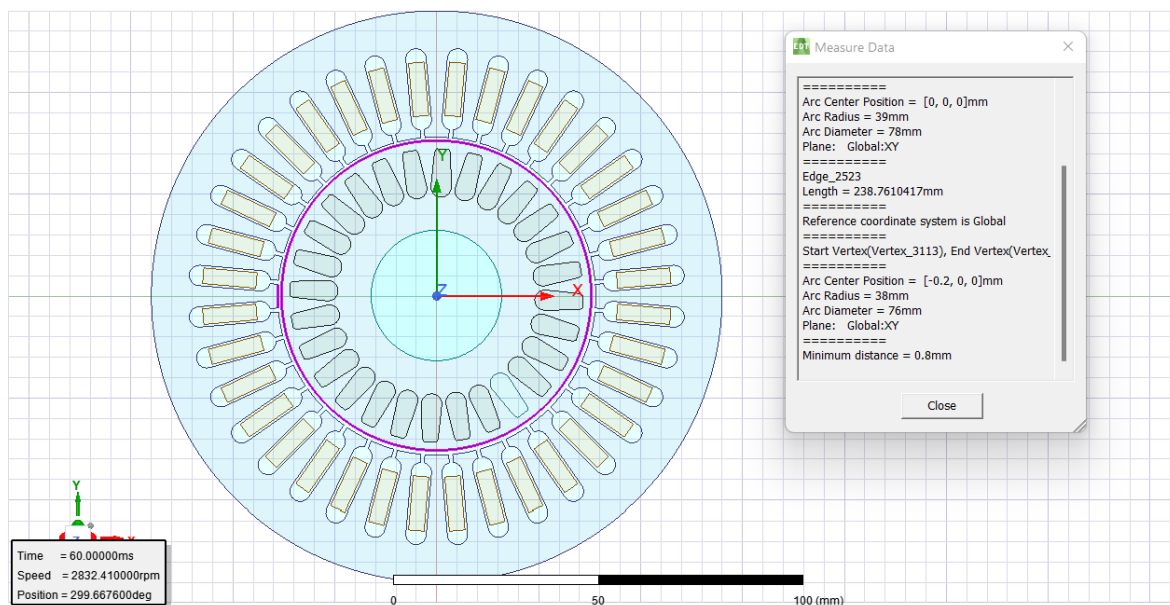


Figure 4.4 Negative x-axis air gap.

To shift the rotor towards negative x-axis, we select Rotor, rotor bars and band, select the move command and move the rotor towards the negative x-axis by putting -0.2mm in x and 0 in y in the cartesian coordinate system. This introduces an air gap of 0.8mm between the rotor and stator on the left side of the model, as shown in the Measure data dialogue box, minimum distance = 0.8mm.

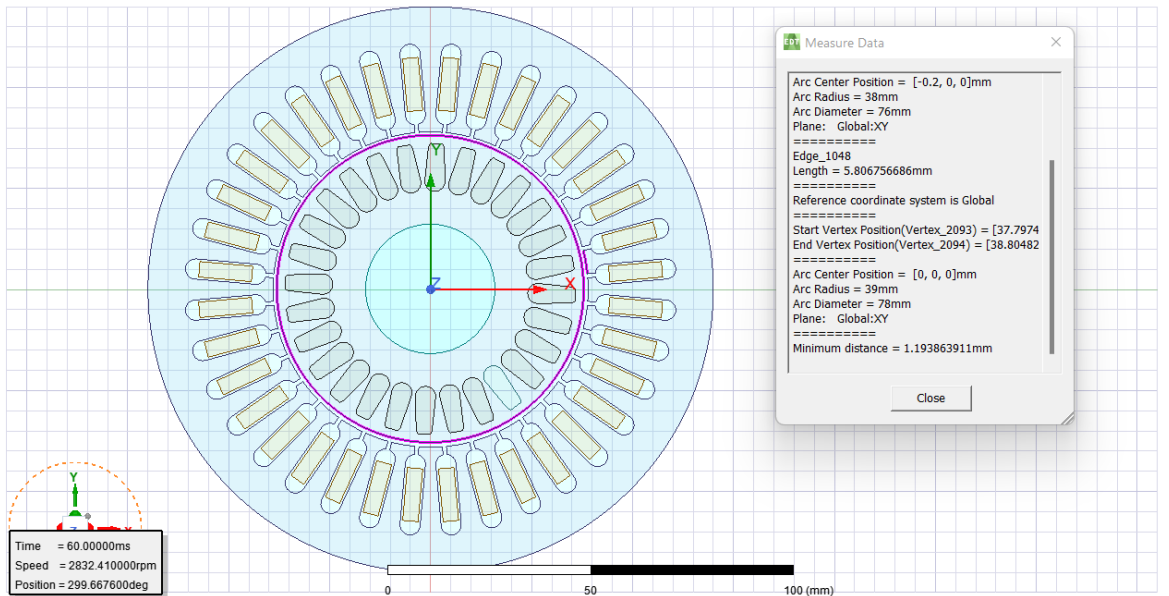


Figure 4.5 Positive x-axis air gap.

The air gap of 1.2mm is introduced between the rotor and stator on the right side of the model, as shown in the Measure data dialogue box, minimum distance = 1.19mm.

The figure 4.6 shows the magnetic flux density distribution in rotor and stator of the induction motor.

Mag_B plot:

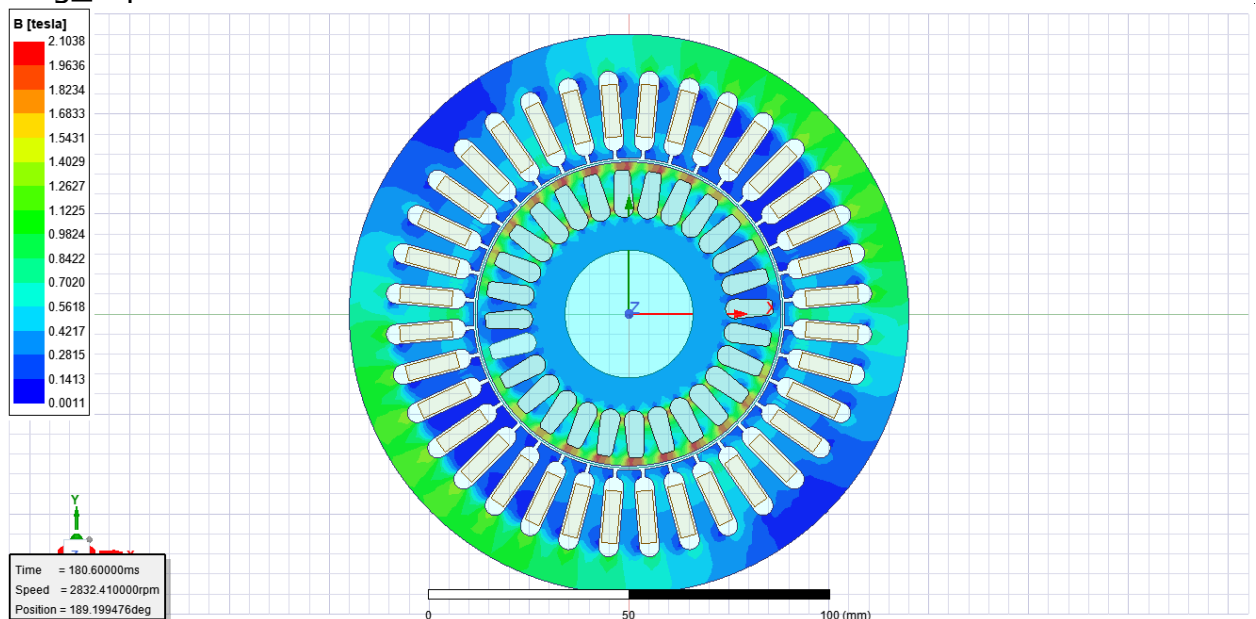


Figure 4.6 Positive x-axis air gap.

2nd case (rotor displaced by 0.1 mm):

A non-uniform air gap of 0.9mm on the positive y-axis and 1.1mm on the negative y-axis, was introduced in the Ansys Maxwell 2D model of the healthy induction motor as shown in figure 4.7 and figure 4.8 respectively.

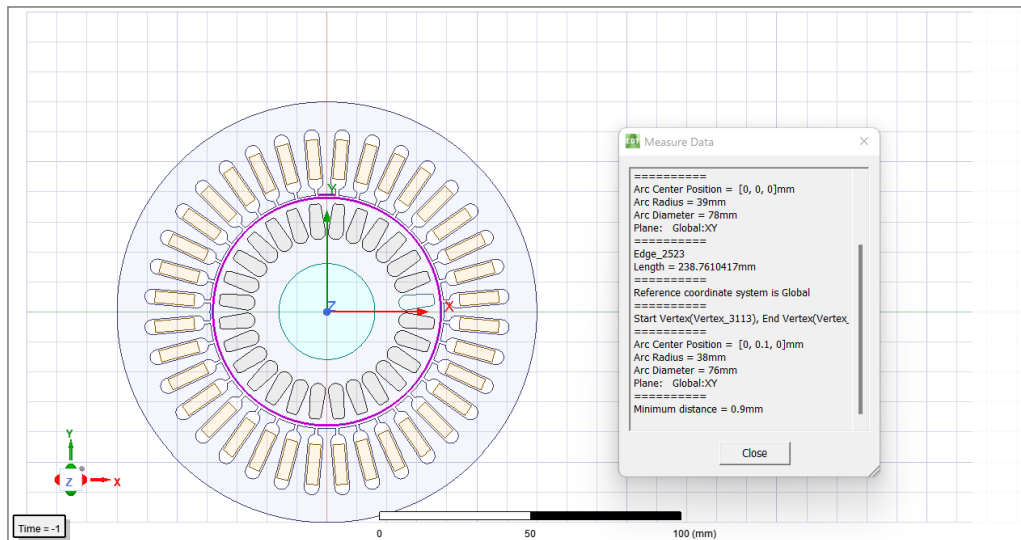


Figure 4.7 Positive y-axis air gap.

To shift the rotor towards positive y-axis, we select Rotor, rotor bars and band, select the move command and move the rotor towards the positive y-axis by putting 0mm in x and 0.1 in y in the cartesian coordinate system. This introduces an air gap of 0.9mm between the rotor and stator on the top side of the model, as shown in the Measure data dialogue box, minimum distance = 0.9mm.

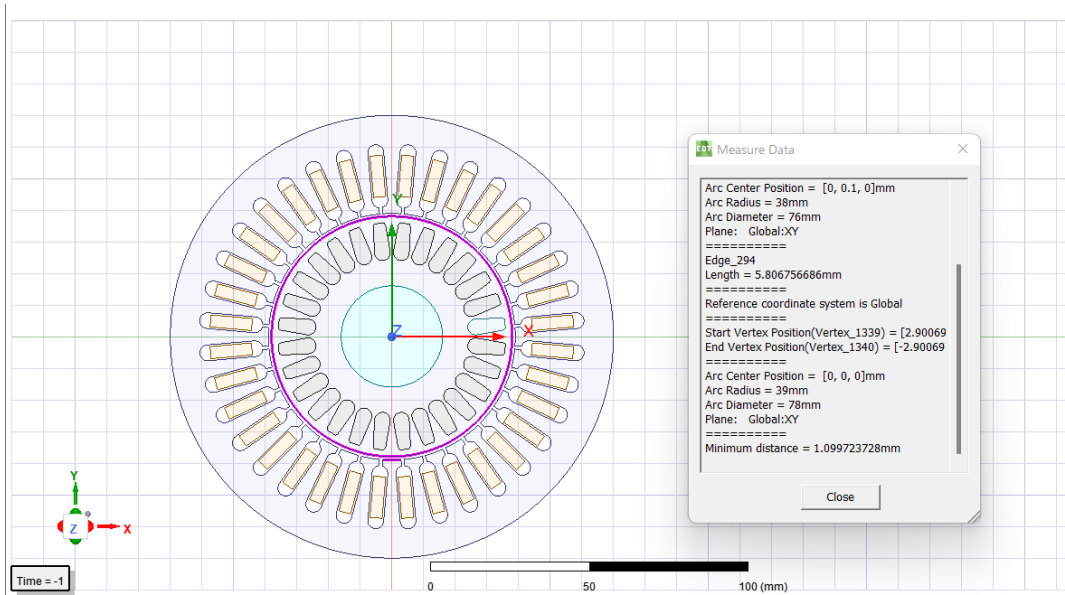


Figure 4.8 Negative y-axis air gap.

The air gap of 1.1mm is introduced between the rotor and stator on the bottom side of the model, as shown in the Measure data dialogue box, minimum distance = 1.09mm.

Mag_B plot:

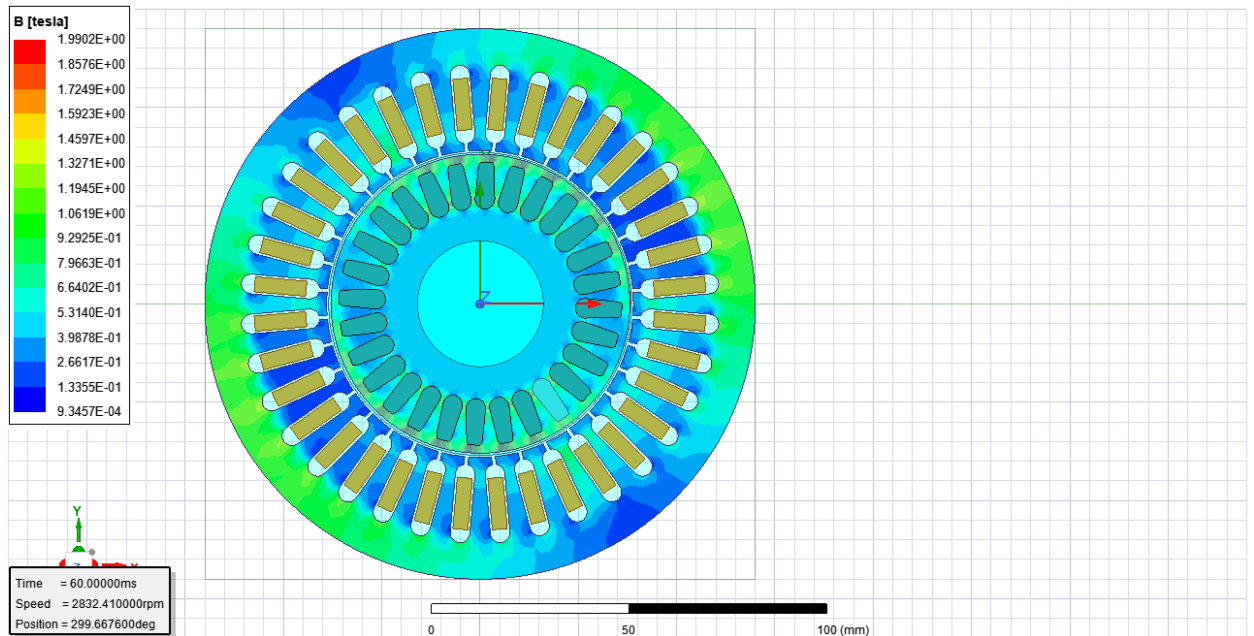


Figure 4.9 Magnetic flux density of faulty motor.

4.3 Mathematical expressions for eccentricity

It is quite an essential and important part to use mathematical expressions to find the eccentricity faults of an IM. The work will be more precise and accurate only if the results of mathematical and simulation results are compared. Certain methods like FFT and FEM are getting more popular in the field of fault diagnosis study. The numerical model of finding the eccentricity is as follows.

4.3.1 Frequency components of the faulty motor

Eccentricity fault

$$f_{ecce} = \left[|kn_b \pm n_d| \left(\frac{1-s}{p} \right) \pm v \right] f_s \quad (4.1)$$

Mixed eccentricity equation:

$$f_{ecce} = f_s \pm kf_r \quad (4.2)$$

$$\text{Dynamic eccentricity} \quad f_{ecce} = f_s \left[k * \left(\frac{1-s}{p} \right) \pm m \right] \quad (4.3)$$

f_{ecce} is the eccentricity frequency, p is the number of poles. v supply fed harmonics and f_s is the supply frequency. s is the slip. n_b is the number of rotor bars and n_d is the dynamic eccentricity (0 for static and 1,2,3....) $k = 1, 2, 3, \dots$, $m = 1, 2, 3, \dots$

5. RESULTS AND DISCUSSIONS

5.1 Transient analysis of Healthy induction motor without load

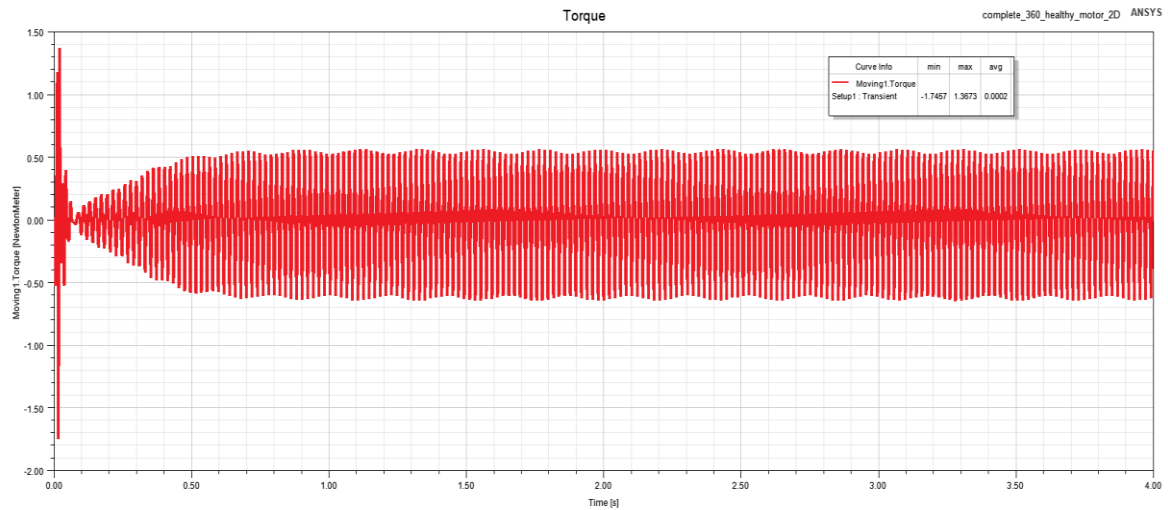


Figure 5.1 Transient analysis of the moving torque.

The figure 5.1 is the transient analysis of moving torque of healthy induction motor with load conditions. The vertical axis shows the moving torque in Nm. The horizontal axis represents the time domain in sec. This red coloured distortion shows the moving torque from the time period of 0 to 4 secs. As we can notice that the moving torque shows a transient behaviour from the initial stage and settle over a period of time. From the time 0.50s, the torque shows a steady state until the end of simulation time. The maximum, minimum and average values are 1.3673, -1.74 and 0.0002.

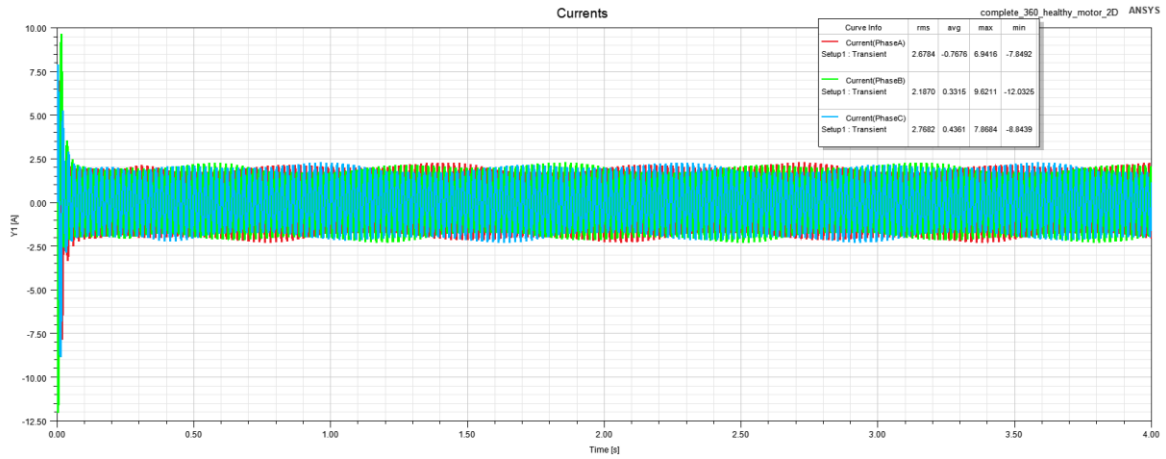


Figure 5.2 Transient analysis of current.

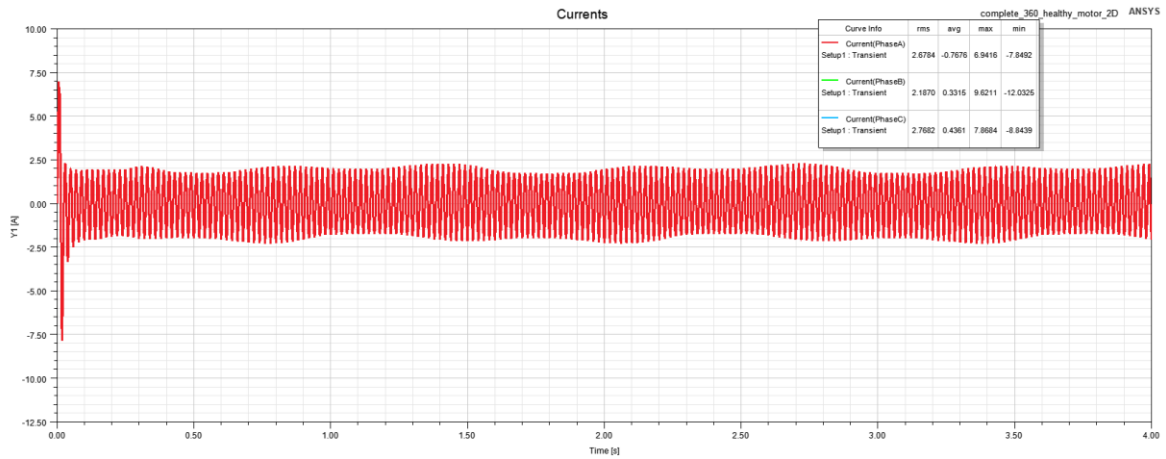


Figure 5.3 Transient analysis of Phase A.

The figure 5.2 is the transient analysis of the current of healthy induction motor with load conditions. The vertical axis shows the current in Ampere. The horizontal axis represents the time domain in sec. The Transient analysis of current in 3 different phases is shown in red, green and blue colours. The maximum, minimum and average values of phase A are 6.9416, -7.6492 and -0.7676, for phase B are 9.6211, -12.0325 and 0.3315, for phase C are 7.8684, -8.88439 and 0.4369.

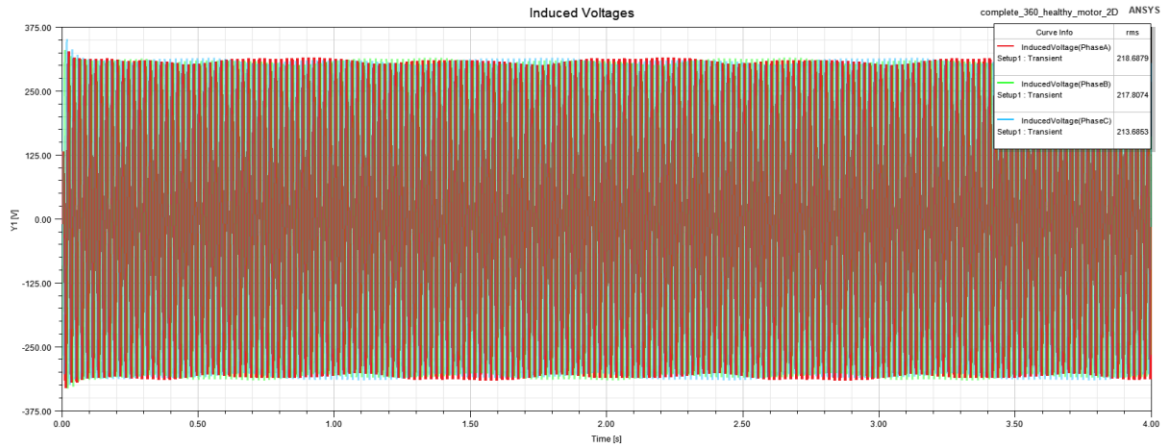


Figure 5.4 Transient analysis of Induced voltage.

The figure 5.4 the transient analysis of the induced voltages of healthy induction motor with load conditions. The vertical axis shows the induced voltage in V. The horizontal axis represents the time domain in sec. The Transient analysis of induced voltage in 3 different phases is shown in red, green and blue colours. The maximum, minimum and average values of phase A are 484.2739, -434.6749 and -0.2136, for phase B 365.8202, -667.4569 and 0.0798, for phase C are 426.3125, -362.3404 and 0.1496

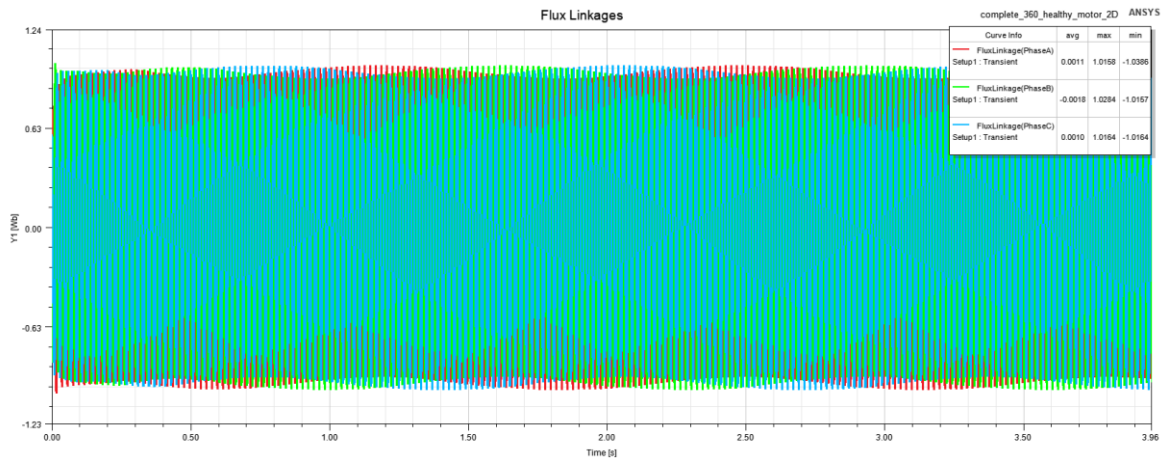


Figure 5.5 Transient analysis of flux linkages.

The figure 5.5 is the transient analysis of the flux linkages of healthy induction motor with load conditions. The vertical axis shows the flux linkages in Wb. The horizontal axis represents the time domain in sec. The Transient analysis of flux linkages in 3 different phases is shown in red, green and blue colours. The maximum, minimum and average values of phase A are 1.0158, -1.0386 and 0.0011, for phase B are 1.0284, -1.0157 and -0.0018, for phase C are 1.0164, -1.0164 and 0.0010.

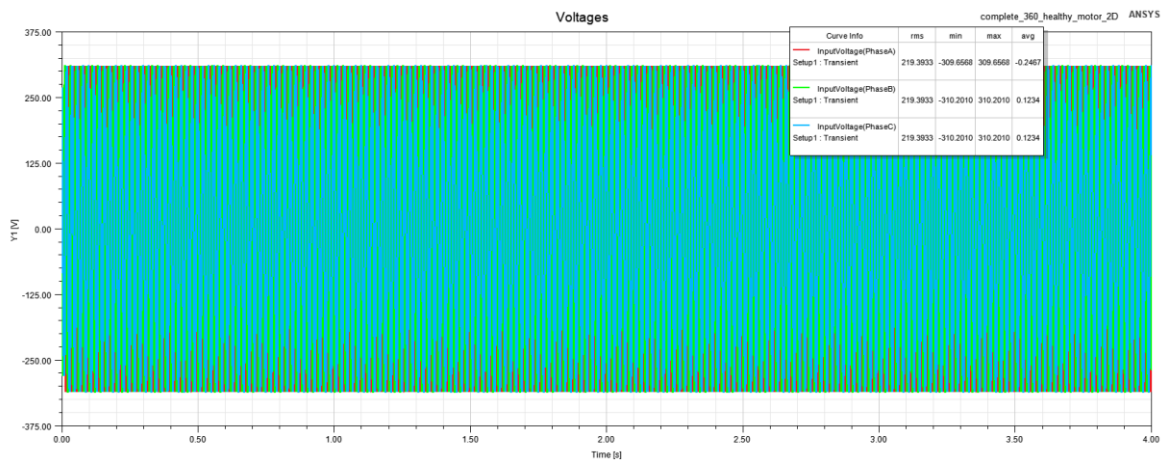


Figure 5.6 Transient analysis of voltages

The figure 5.6 is the transient analysis of the voltages of healthy induction motor with load conditions. The vertical axis shows the voltage in V. The horizontal axis represents the time domain in sec. The Transient analysis of voltage in 3 different phases is shown in red, green and blue colours. The maximum, minimum and average values of phase A are 309.6558, -309.6558 and -0.2467, for phase B are 310.2010, -310.2010 and 0.1234, for phase C are 310.2010, -310.2010 and 0.1234.

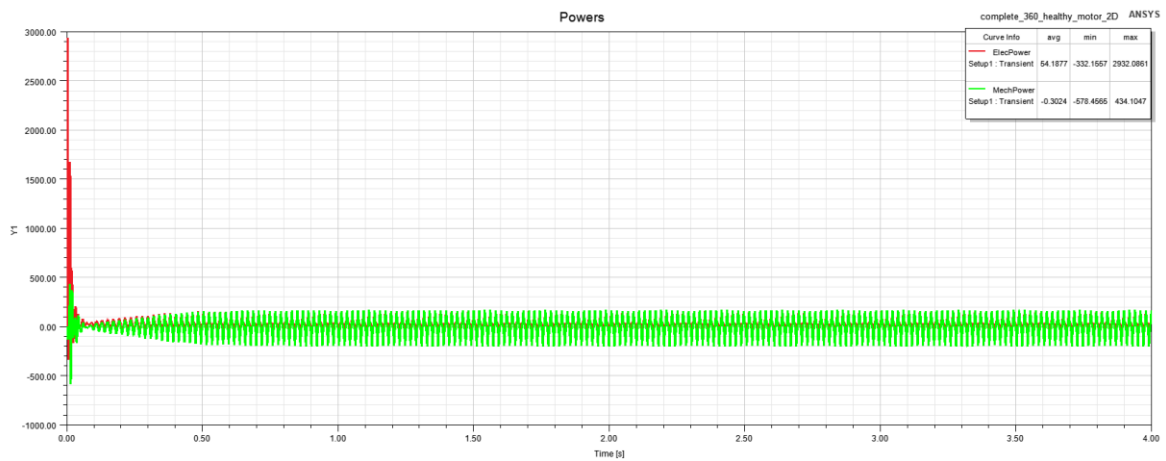


Figure 5.7 Transient analysis of power

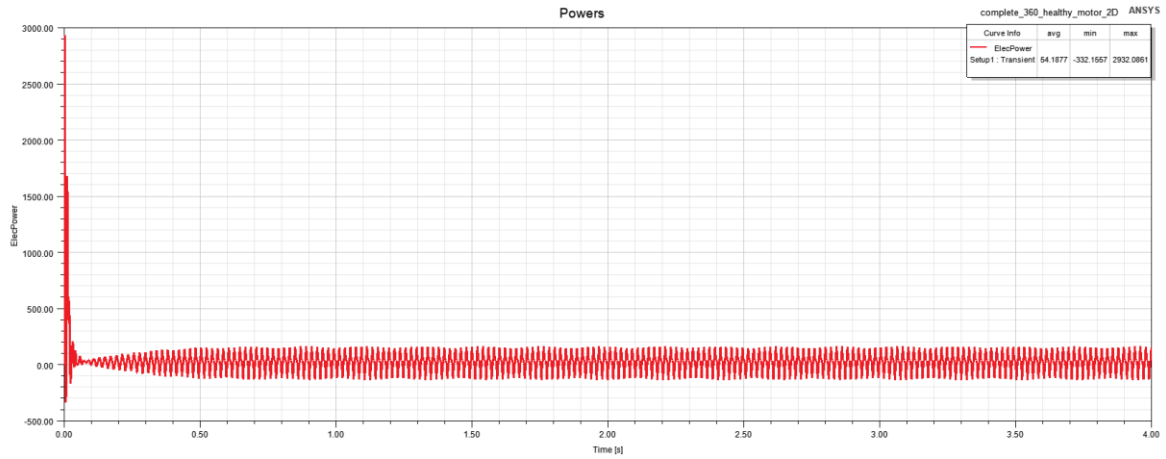


Figure 5.8 Transient analysis of power

The figure 5.8 is the transient analysis of the electrical and mechanical power of healthy induction motor with load conditions. The vertical axis shows the electrical and mechanical power. The horizontal axis represents the time domain in sec. The Transient analysis of electrical and mechanical power is shown in red and green colour. The maximum, minimum and average values of electrical power are 2932.0861, -332.1557 and 54.1887. The maximum, minimum and average values of mechanical power are 434.1047, -578.4565 and -0.3024.

5.2 Transient analysis of Healthy induction motor with load

Figure 5.9 shows the moving torque graph with respect to time. Here, time is a variable that we have put in the Ansys Maxwell 2D Transient simulation solution setup.

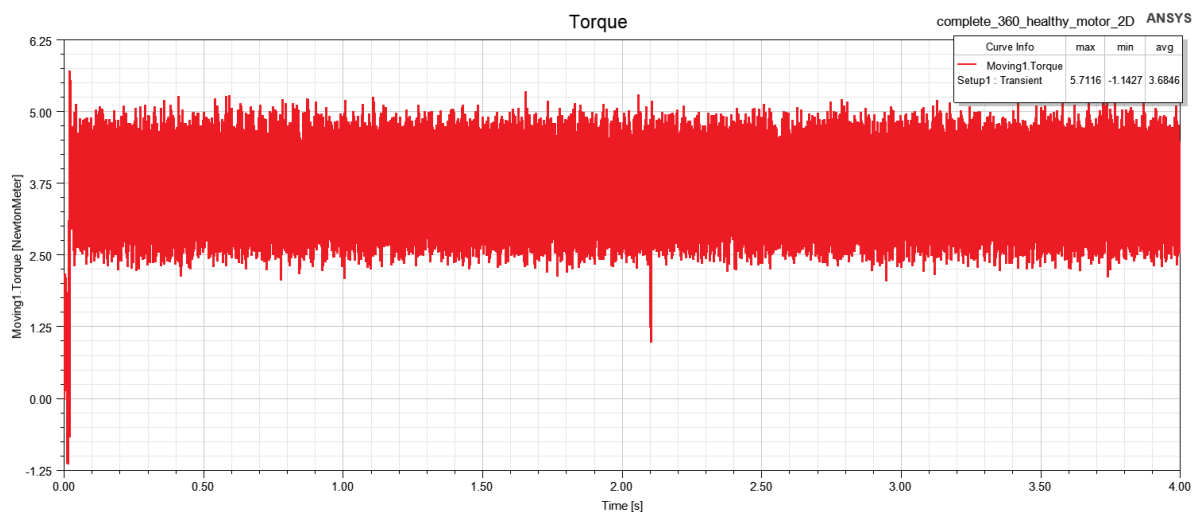


Figure 5.9 Transient analysis of the moving torque

The figure 5.9 the transient analysis of movie torque of a healthy induction motor with load conditions. The vertical axis shows the moving torque in Nm. The horizontal axis represents the time domain in sec. This red coloured distortion shows the moving torque from the time period of 0 to 4 secs. As we can notice, the moving torque shows a transient behaviour from the initial stage and settle over time. From the time 0.50s, the torque shows a steady state until the end of simulation time. The maximum, minimum and average values are 5.7116, -1.1427 and 3.6846.

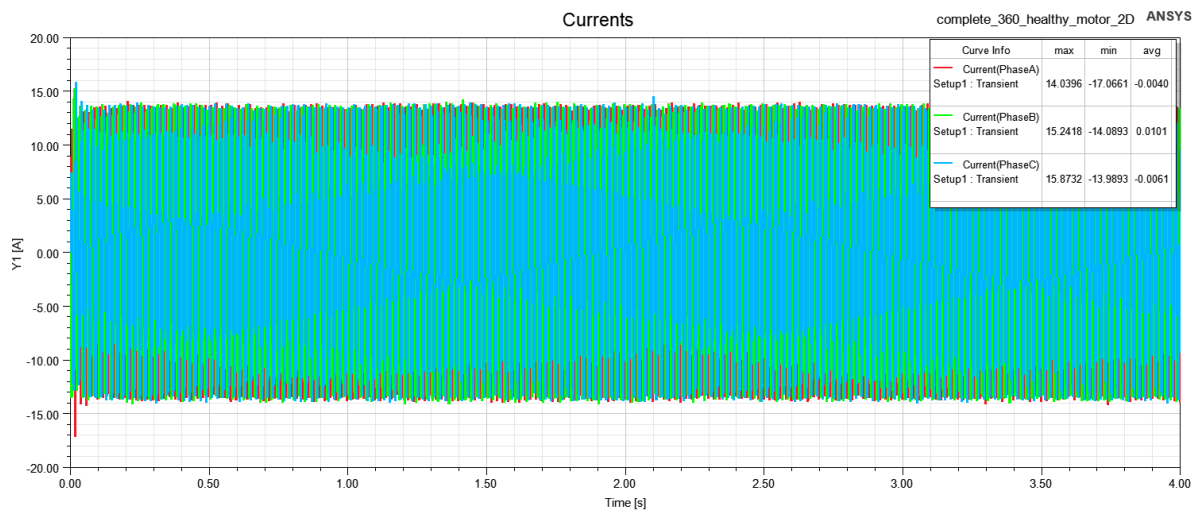


Figure 5.10 Transient analysis of current

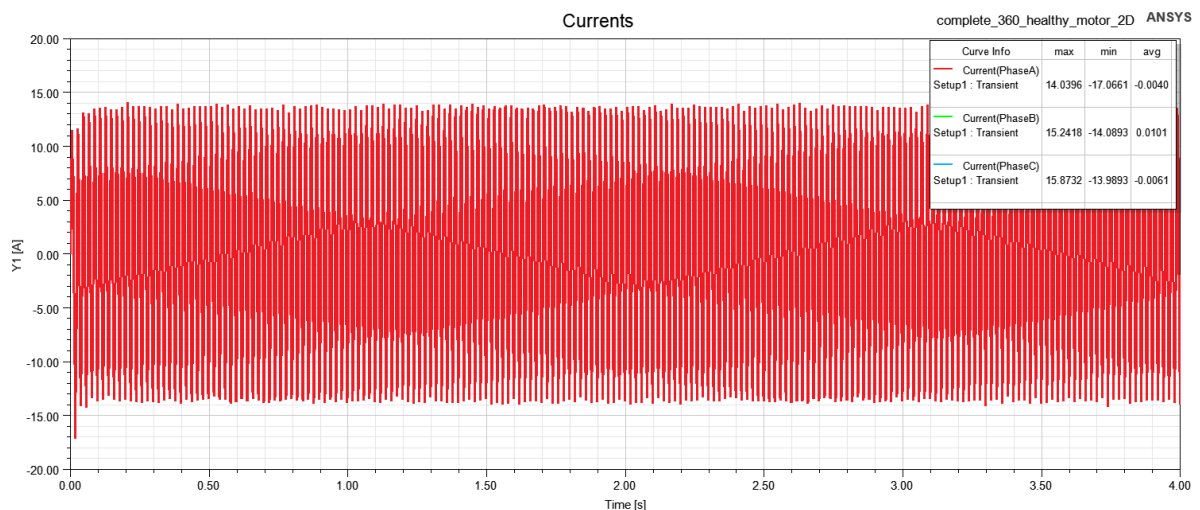


Figure 5.11 Transient analysis of Phase A

The figure 5.10 is the transient analysis of the current of a healthy induction motor with load conditions. The vertical axis shows the current in Ampere. The horizontal axis

represents the time domain in sec. The Transient analysis of current in 3 different phases is shown in red, green and blue colours. The maximum, minimum and average values of phase A are 14.0396, -17.0661 and -0.0040, for phase B are 15.2418, -14.0893 and 0.0101, for phase C are 15.8732, -13.9893 and -0.0061.

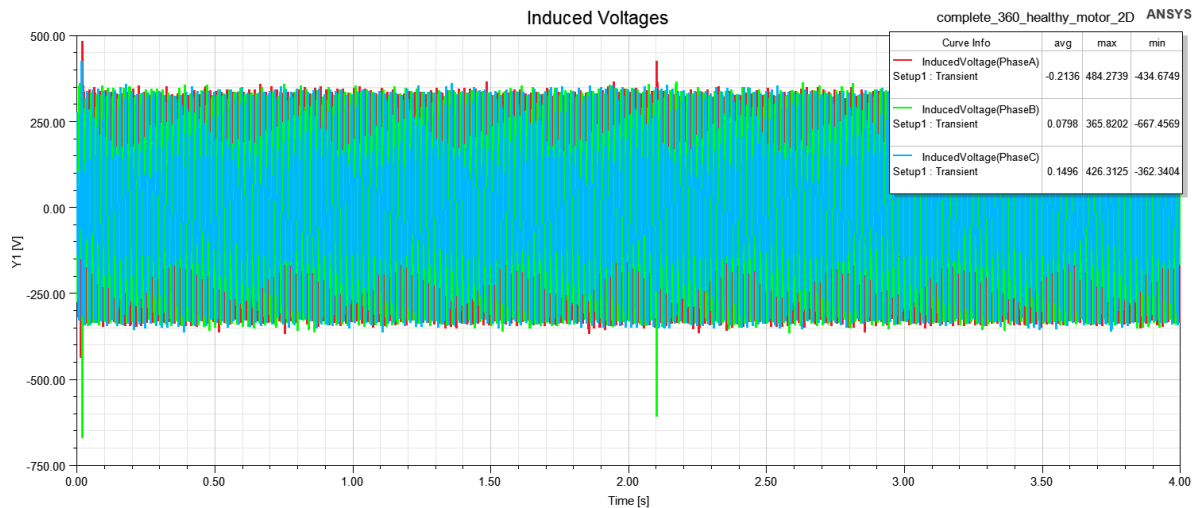


Figure 5.12 Transient analysis of induced voltages

The figure 5.12 is the transient analysis of the induced voltages of a healthy induction motor with load conditions. The vertical axis shows the induced voltage in V. The horizontal axis represents the time domain in sec. The Transient analysis of induced voltage in 3 different phases is shown in red, green and blue colours. The maximum, minimum and average values of phase A are 484.2739, -434.6749 and -0.2136, for phase B 365.8202, -667.4569 and 0.0798, for phase C are 426.3125, -362.3404 and 0.1496.

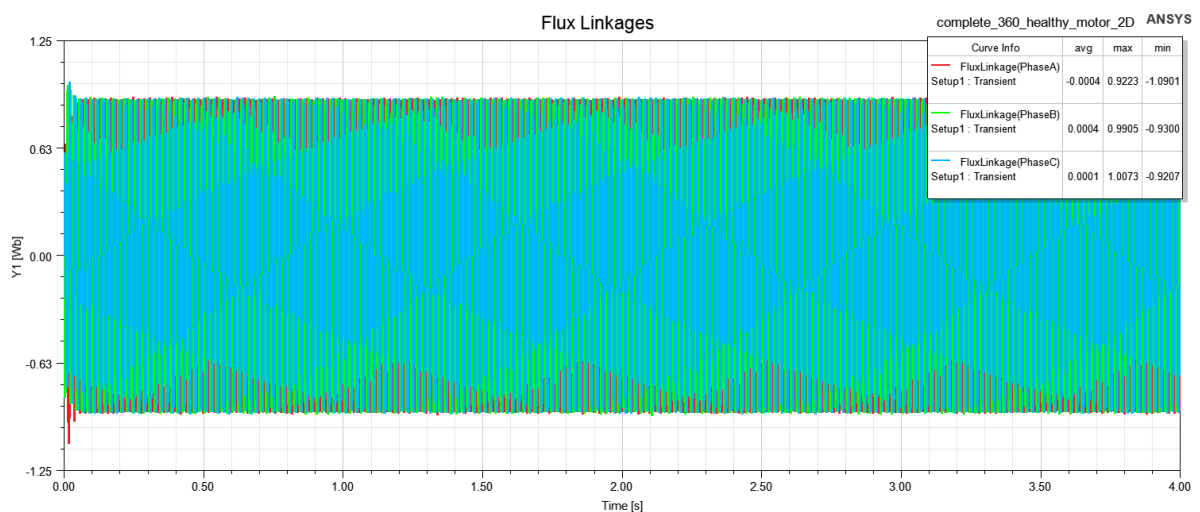


Figure 5.13 Transient analysis of flux linkages

The figure 5.13 shows the transient analysis of the flux linkages of a healthy induction motor with load conditions. The vertical axis shows the flux linkages in Wb. The horizontal axis represents the time domain in sec. The Transient analysis of flux linkages in 3 different phases is shown in red, green and blue colours. The maximum, minimum and average values of phase A are 0.9223, -1.0901 and -0.0004, for phase B are 0.9905, -0.9300 and 0.0004, for phase C are 1.0073, -0.9207 and 0.0001

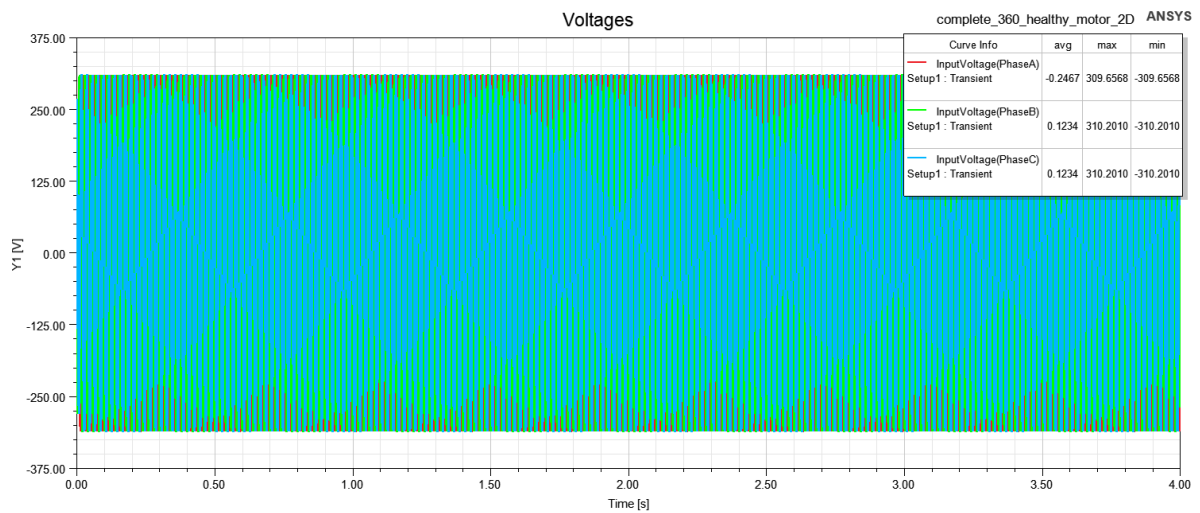


Figure 5.14 Transient analysis of voltages

The figure 5.14 shows the transient analysis of the voltages of healthy induction motor with load conditions. The vertical axis shows the voltage in V. The horizontal axis represents the time domain in sec. The Transient analysis of voltage in 3 different phases is shown in red, green and blue colours. The maximum, minimum and average values of phase A are 309.6568, -309.6568 and -0.2467, for phase B are 310.2010, -310.2010 and 0.1234, for phase C are 310.2010, -310.2010 and 0.1234.

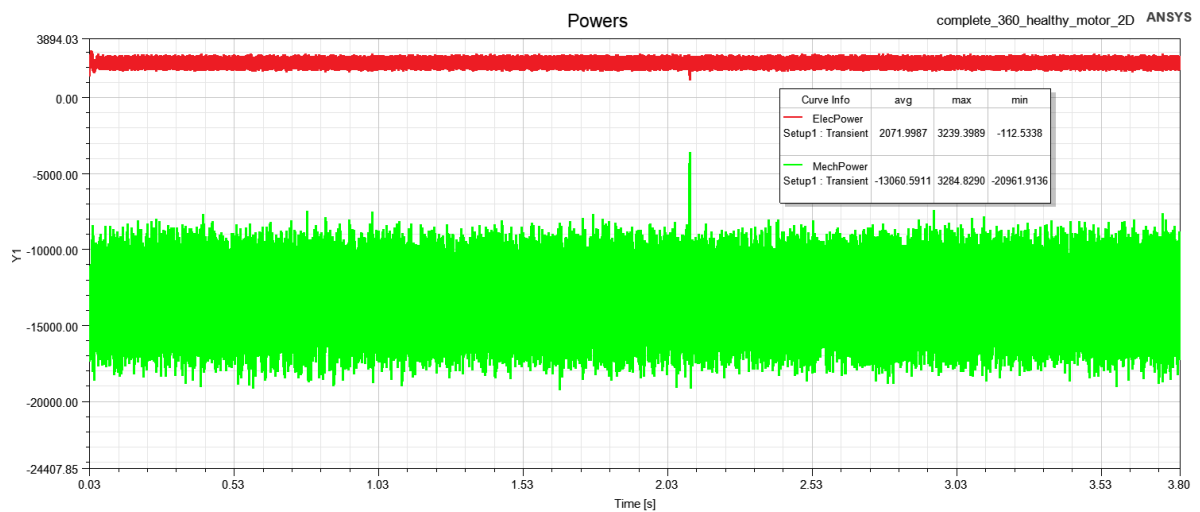


Figure 5.15 Transient analysis of powers

The figure 5.15 is the transient analysis of the electrical and mechanical power of a healthy induction motor with load conditions. The vertical axis shows the electrical and mechanical power. The horizontal axis represents the time domain in sec. The Transient analysis of electrical and mechanical power is shown in red and green colour. The maximum, minimum and average values of electrical are 3239.3989, -112.5338 and 2071.9987, for mechanical are. 3284.8290, -20961.9136, and -13060.5911.

5.3 Transient analysis of Faulty induction motor without load.

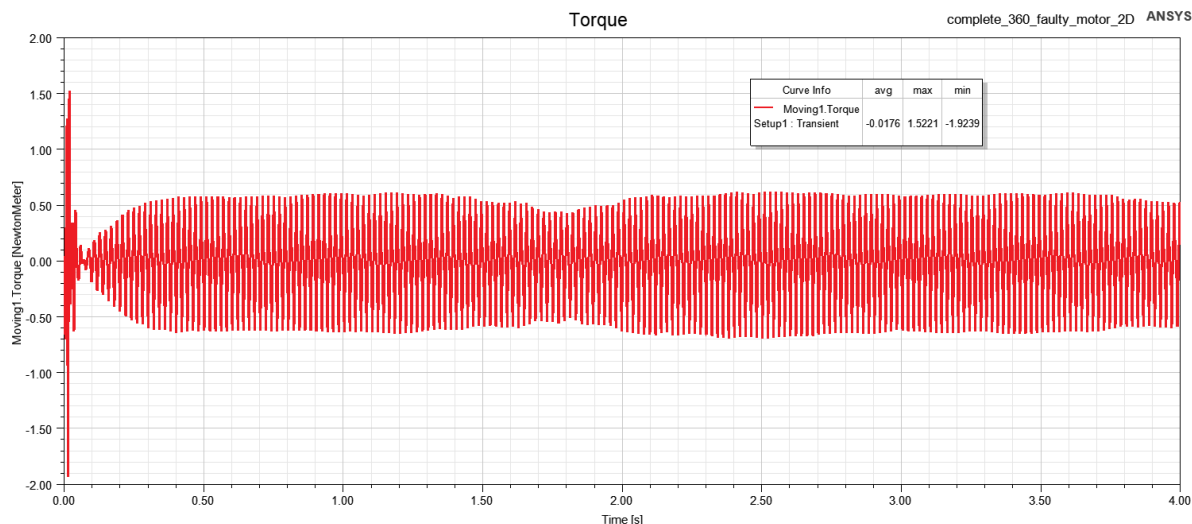


Figure 5.16 Transient analysis of the moving torque

The figure 5.16 is the transient analysis of movie torque of healthy induction motor with load conditions. The vertical axis shows the moving torque in Nm. The horizontal axis represents the time domain in sec. This red coloured distortion shows the moving torque from the time period of 0 to 4 secs. As we can notice, the moving torque shows a transient behaviour from the initial stage and settle over time. From the time 0.50s, the torque shows a steady state until the end of simulation time. The maximum, minimum and average values are 1.5221, -1.9239 and -0.0176.

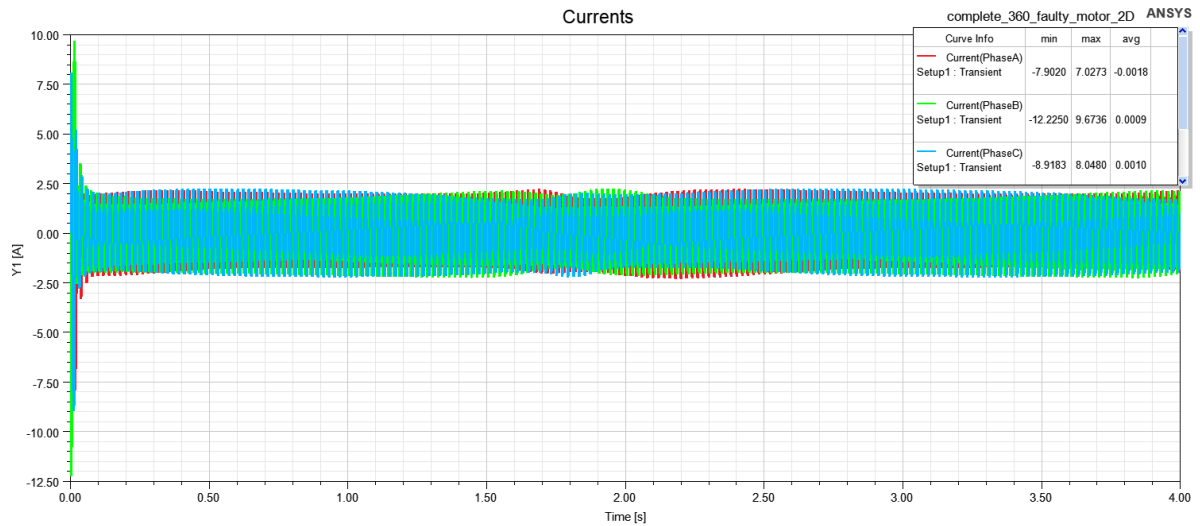


Figure 5.17 Transient analysis of current

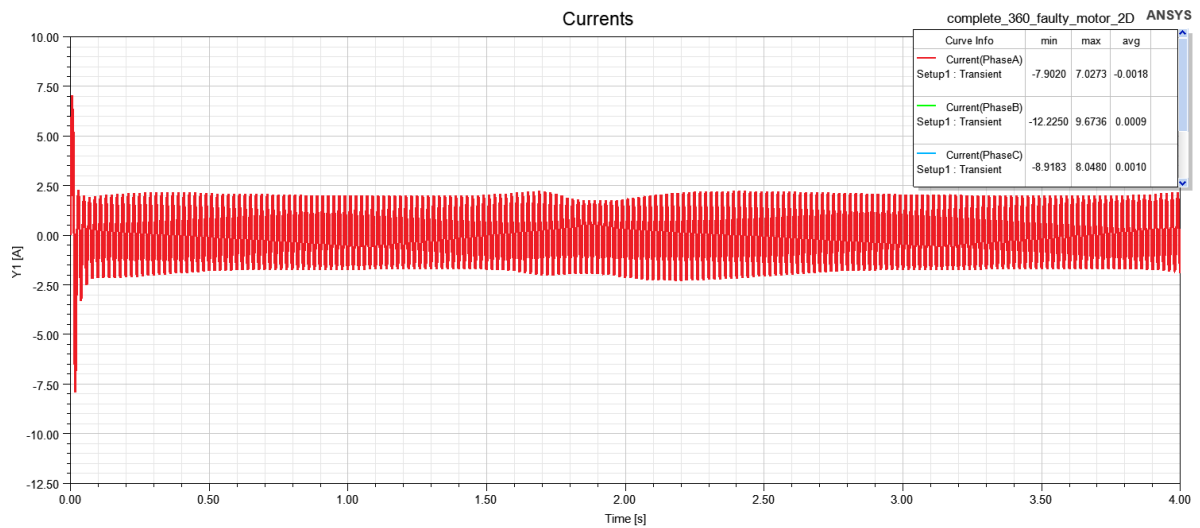


Figure 5.18 Transient analysis of phase A.

The figure 5.18 is the transient analysis of the current of a healthy induction motor with load conditions. The vertical axis shows the current in Ampere. The horizontal axis represents the time domain in sec. The Transient analysis of current in 3 different phases is shown in red, green and blue colours. The maximum, minimum and average values of phase A are 7.0273, -7.9020 and -0.0018, for phase B are 9.6736, -12.2250 and 0.0009, for phase C are 8.0480, -8.9183 and 0.0010.

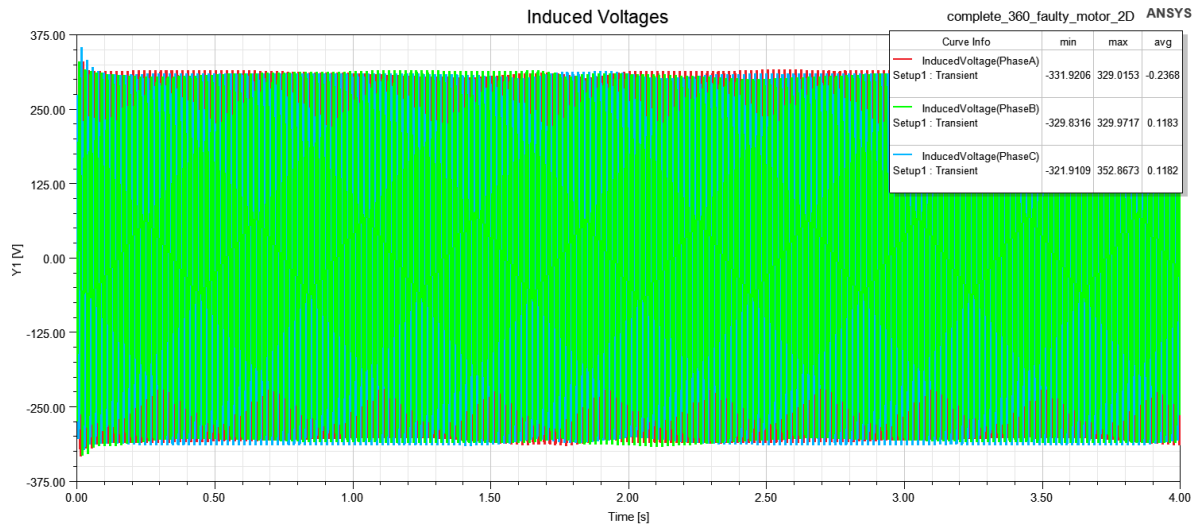


Figure 5.19 Transient analysis of induced voltages.

The figure 5.19 is the transient analysis of the induced voltages of a healthy induction motor with load conditions. The vertical axis shows the induced voltage in V. The horizontal axis represents the time domain in sec. The Transient analysis of induced voltage in 3 different phases is shown in red, green and blue colours. The maximum, minimum and average values of phase A are 329.0153, -331.9206 and -0.2368, for phase B 329.9717, -329.6316, 0.1183, for phase C are 352.8673, -321.9109 and 0.1182.

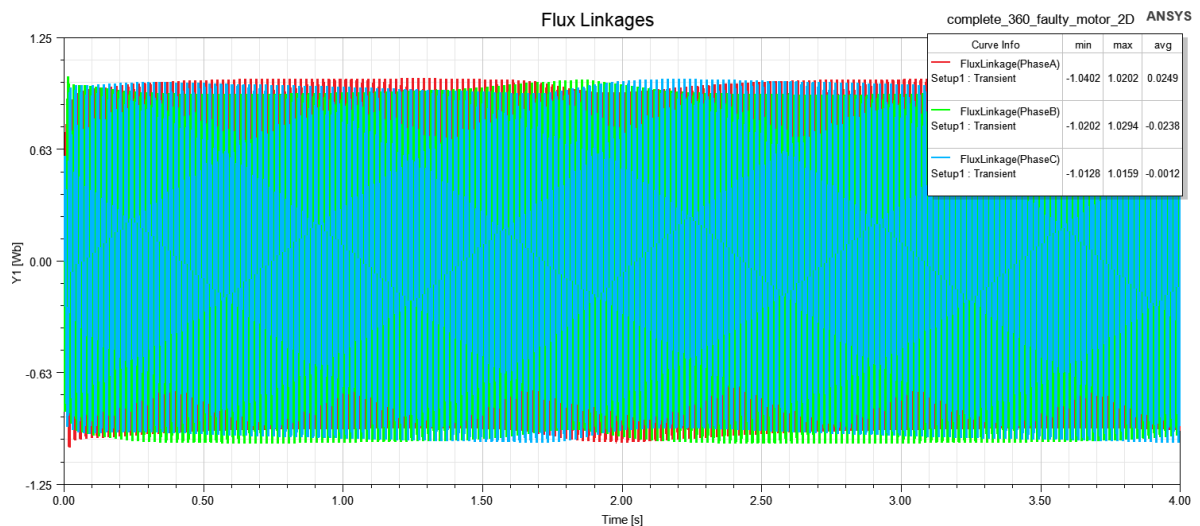


Figure 5.20 Transient analysis of flux linkages.

The figure 5.20 is the transient analysis of the flux linkages of a healthy induction motor with load conditions. The vertical axis shows the flux linkages in Wb. The horizontal axis

represents the time domain in sec. The Transient analysis of flux linkages in 3 different phases is shown in red, green and blue colours. The maximum, minimum and average values of phase A are 1.0202, -1.0402 and 0.0249, for phase B are 1.0294, -1.0202 and -0.0238, for phase C are 1.0159, -1.0128 and -0.0012.

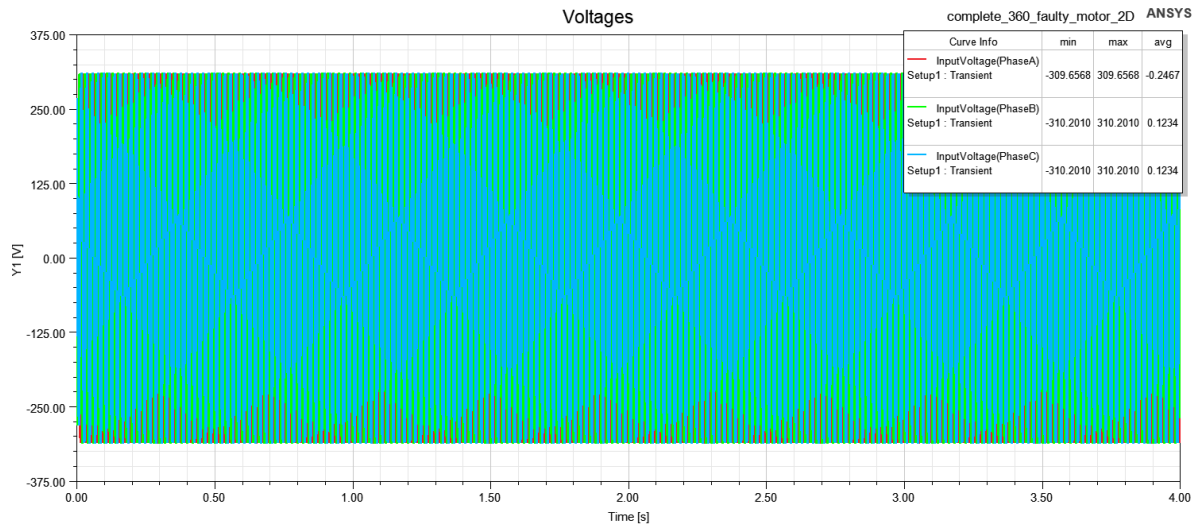


Figure 5.21 Transient analysis of voltages.

The figure the transient analysis of the voltages of a healthy induction motor with load conditions. The vertical axis shows the voltage in V. The horizontal axis represents the time domain in sec. The Transient analysis of voltage in 3 different phases is shown in red, green and blue colours. The maximum, minimum and average values of phase A are 309.6568, -309.6568 and -0.2467, for phase B are 310.2010, -310.2010 and 0.1234, for phase C are 310.2010, -310.2010 and 0.1234.

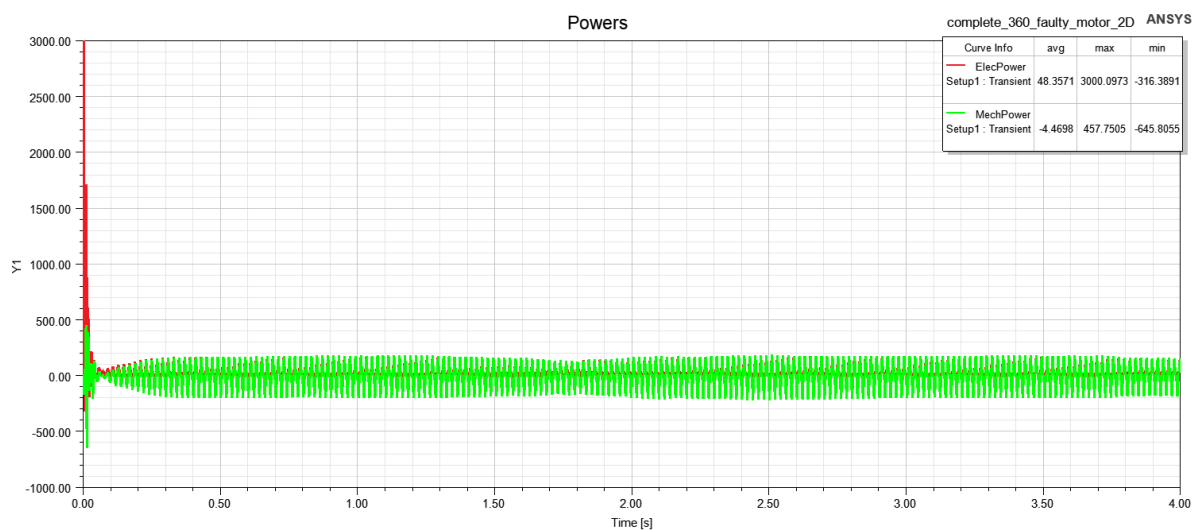


Figure 5.22 Transient analysis of powers.

The figure the transient analysis of the electrical and mechanical power of a healthy induction motor with load conditions. The vertical axis shows the electrical and mechanical power. The horizontal axis represents the time domain in sec. The Transient analysis of electrical and mechanical power is shown in red and green colour. The maximum, minimum and average values of electrical power are 3000.0973, -316.3891 and 48.3571. The maximum, minimum and average values of mechanical power are 457.7505, -645.8055 and -4.4698.

5.4 Transient analysis of Faulty induction motor with load.

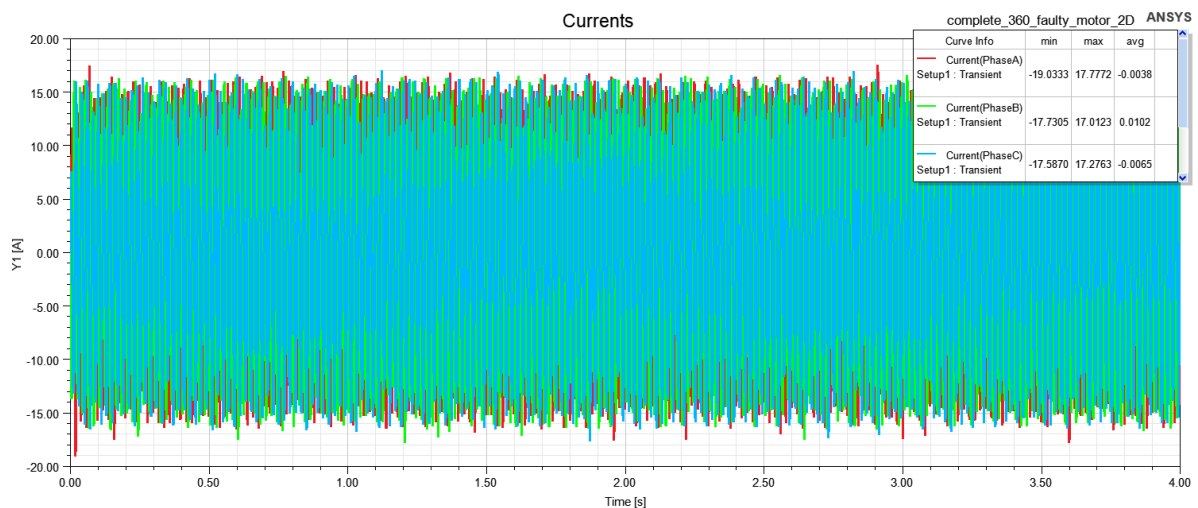


Figure 5.23 Transient analysis of current.

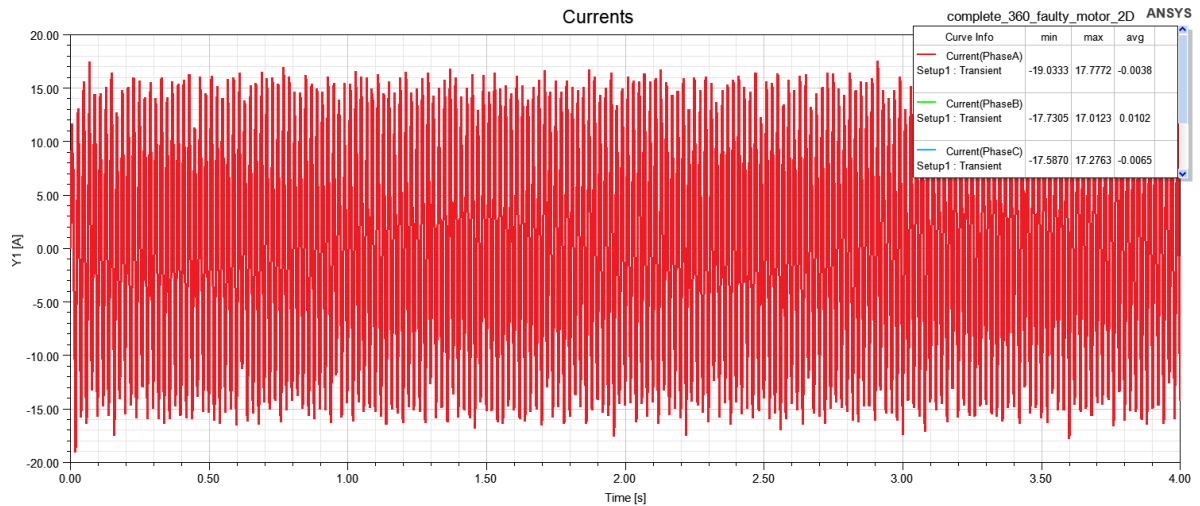


Figure 5.24 Transient analysis of phase A.

The figure 5.23 is the transient analysis of the current of a healthy induction motor with load conditions. The vertical axis shows the current in Ampere. The horizontal axis represents the time domain in sec. The Transient analysis of current in 3 different phases is shown in red, green and blue colours. The maximum, minimum and average values of phase A are 17.7772, -19.033 and -0.0038, for phase B are 17.0123, -17.7305 and 0.0102, for phase C are 17.2763, -17.5870 and -0.0065.

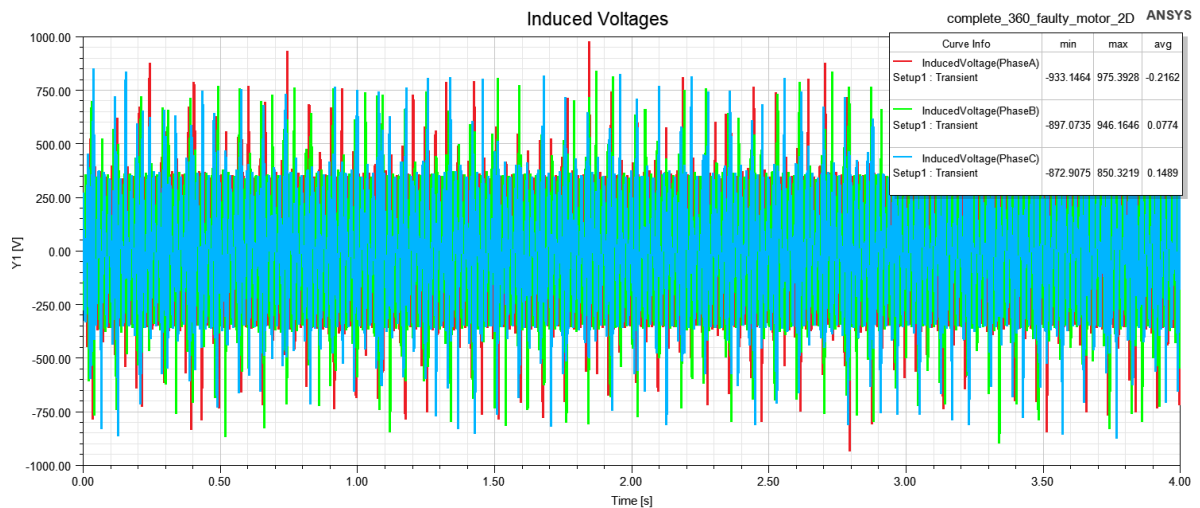


Figure 5.25 Transient analysis of induced voltages.

The figure 5.25 is the transient analysis of the induced voltages of a healthy induction motor with load conditions. The vertical axis shows the induced voltage in V. The horizontal axis represents the time domain in sec. The Transient analysis of induced voltage in 3 different phases is shown in red, green and blue colours. The maximum, minimum and average values of phase A are 975.3928, -933.1464 and -1.2162, for

phase B 946.1646, -897.0735 and 0.0074, for phase C are 850.3219, -872.9075 and 0.1489.

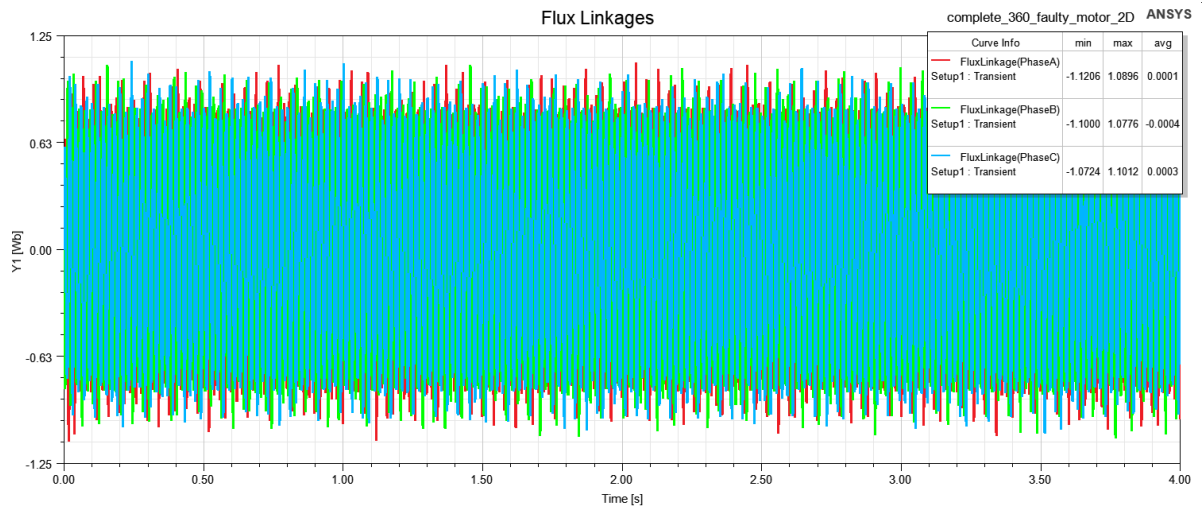


Figure 5.26 Transient analysis of flux linkages.

The figure 5.26 the transient analysis of the flux linkages of a healthy induction motor with load conditions. The vertical axis shows the flux linkages in Wb. The horizontal axis represents the time domain in sec. The Transient analysis of flux linkages in 3 different phases is shown in red, green and blue colours. The maximum, minimum and average values of phase A are 1.0896, -1.1206 and 0.0001, for phase B are 1.0776, -1.1000 and -0.0004, for phase C are 1.1012, -1.0724 and 0.0003.

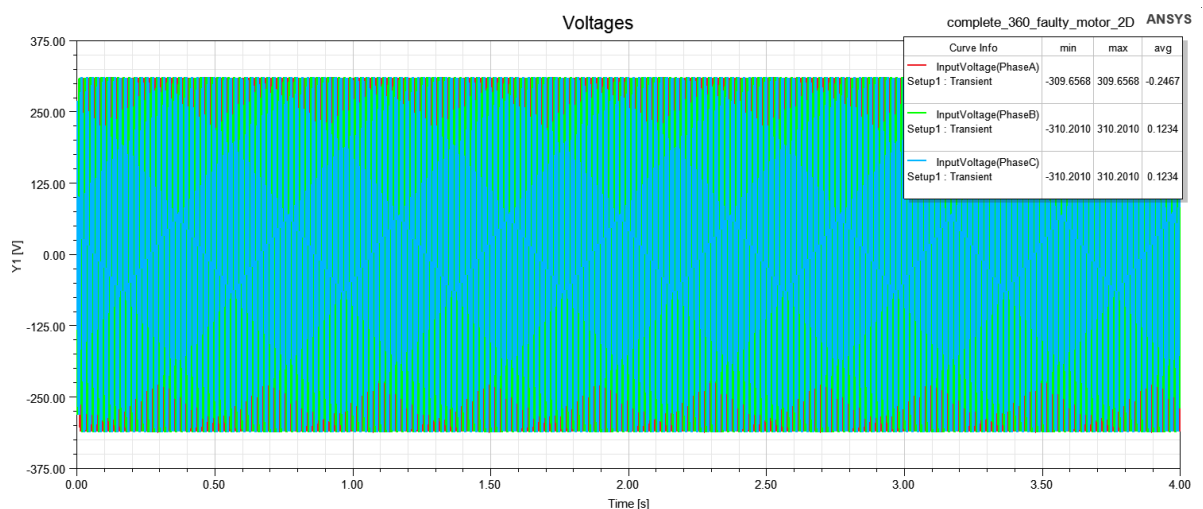


Figure 5.27 Transient analysis of voltages.

The figure 5.27 the transient analysis of the voltages of a healthy induction motor with load conditions. The vertical axis shows the voltage in V. The horizontal axis represents the time domain in sec. The Transient analysis of voltage in 3 different phases is shown in red, green and blue colours. The maximum, minimum and average values of phase A are 309.6568, -309.6568 and -0.2467, for Phase B are 310.2010, -310.2010 and 0.1234, for phase C are 310.2010, -310.2010 and 0.1234

5.6 Co-simulation of Ansys and Matlab

The results generated after the transient analysis in Ansys had been exported to the excel format. The Transient analysis of all the parameters including Torque, current and induced voltage, has been exported. A program code has been written in Matlab to plot the Fast Fourier transform (FFT) of the given parameters in a logarithmic scale.

```
t = csvread('Healthy_withload_Currents.csv');

%sample rate
dt = 0.0004;
fs = 1/dt;

%time domain signal
figure
plot(t(initial:final,2));

t=t(initial:final,2);
t_f=fft(t);
m = length(t_f);
freq = (-m/2:(m/2-1))*fs/(m-1);

figure
semilogx(freq,fftshift(abs(t_f)));
```

The Matlab program to plot the FFT analysis is shown above. The transient analysis results verified the motor's transient behaviour and steady state behaviour in load and no-load conditions. Both the healthy and faulty models have tested in the load conditions. From the results, verifying the torque variations in the motor, the initial and final steps were taken for the FFT analysis. The steady state time period is given as,

```

t = csvread('Healthy_withload_Currents.csv');

%sample rate
dt = 0.0004;
fs =1/dt;

%time domain signal
figure
plot(t(2500:5001,2));

t=t(2500:5001,2);
t_f=fft(t);
m = length(t_f);
freq = (-m/2:(m/2-1))*fs/(m-1);

figure
semilogx(freq,fftshift(abs(t_f)));

```

5.7 FFT analysis of motor in load conditions

After the simulation of both the models, the results were exported in the format of excel. So, with the help of the Matlab program, the FFT analysis should be analysed. For that, here steady state of the simulation was taken. By checking the torque graphs, the point at which the motor gets into the steady state from the transient state was noticed. The portion that I required for the FFT analysis is separated from the data collected from Ansys.

In this analysis, the comparison is done for the faulty and healthy model in load conditions, and the generated graph of current are analysed for fault detection. For that, the missing frequency component will be shown in a table and the resulted data is validated accordingly with the eccentricity equations.

Faulty motor:

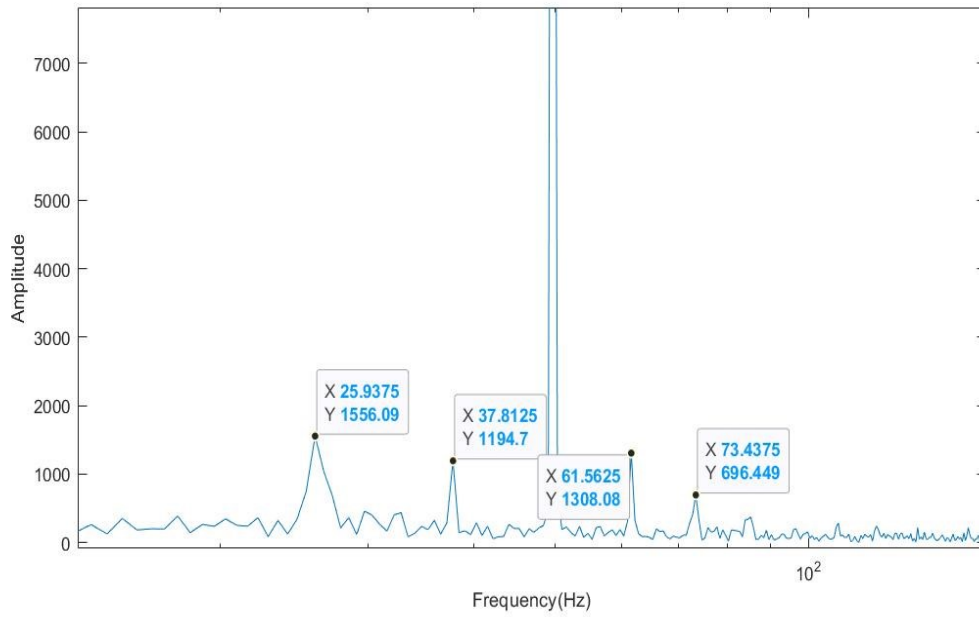


Figure 5.28 Faulty motor with load conditions.

The figure 5.29 shows the FFT analysis of faulty motor, plotted with respect to frequency time domain variants. The x-axis represents the frequency in time domain, y-axis represents the amplitude.

Healthy motor:

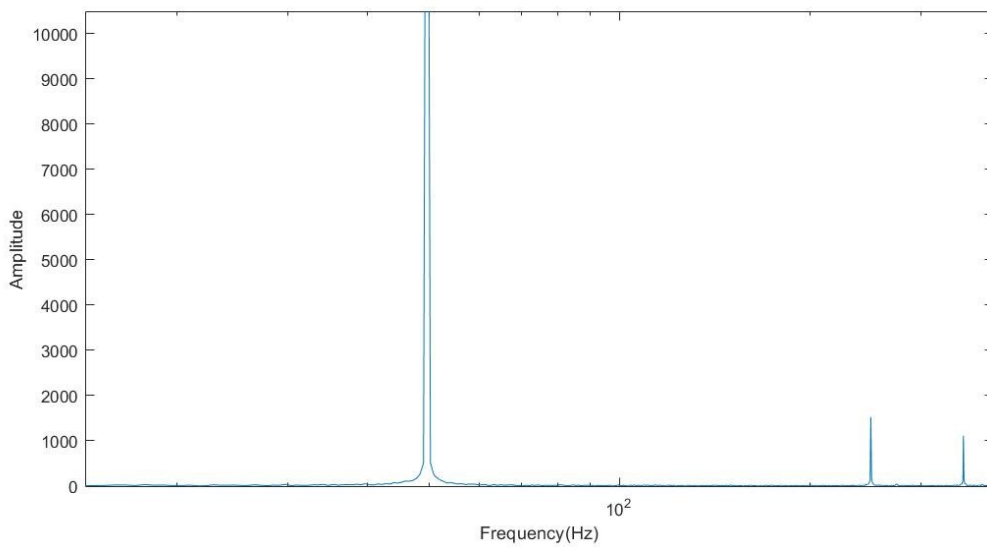


Figure 5.290 Healthy motor with load conditions.

The figure 5.30 shows the FFT analysis of faulty motor, plotted with respect to frequency time domain variants. The x-axis represents the frequency in time domain, whereas y-axis represents the amplitude.

Table 5.1 Validation of frequency component in steady state.

PARAMETERS	HEALTHY		FAULTY		FEccentricity(eqn)
	Frequency(Hz)	Amplitude	Frequency(Hz)	Amplitude	
CURRENT(A)	Not present	Not present	25.9375	1556.09	22
	Not present	Not present	37.8125	1194.7	38.8
	Not present	Not present	61.5625	1308.08	62.4
	Not present	Not present	73.4375	696.449	73.3

Validation with the eccentricity equation:

$$\text{Dynamic eccentricity} \quad f_{ecce} = f_s \left[k * \left(\frac{1-s}{p} \right) \pm m \right]$$

where f_{ecce} is the supply frequency with 50Hz, S is the slip value 0.056, p is the number of poles 2 and where k and m = 1,2,3,.....

$$1. \quad f_{ecce} = f_s \left[k * \left(\frac{1-s}{p} \right) \pm m \right]$$

$$K= 20, s= 0.056, m=-9, p=2$$

$$f_{ecce} = 22 \text{ Hz}$$

$$2. \quad f_{ecce} = f_s \left[k * \left(\frac{1-s}{p} \right) \pm m \right]$$

$$K= 8, s= 0.056, m=-3, p=2$$

$$f_{ecce} = 38.8 \text{ Hz}$$

$$3. f_{ecce} = f_s \left[k * \left(\frac{1-s}{p} \right) \pm m \right]$$

$$K= 9, s= 0.056, m=-3 , p=2$$

$$f_{ecce} = 62.4 \text{ Hz}$$

$$4. f_{ecce} = f_s \left[k * \left(\frac{1-s}{p} \right) \pm m \right]$$

$$K= 1, s= 0.056, m=1 , p=2$$

$$f_{ecce} = 73.3 \text{ Hz}$$

The results generated from the equation is given in the table above.

The plotted figures have been provided from the FFT analysis in load conditions in the figure. It can be seen that different frequencies are generated in the faulty motor compared to the healthy one. The frequency and amplitude generated in faulty one are given in the above table 5.1. The healthy and faulty without load conditions have also been plotted for frequency comparison. Since there is not much difference in both models, only the load conditions are considered here. Thus from the methodology of Time-frequency analysis for the eccentricity detection from the healthy and faulty motors, it is possible to determine the consistency of the engine in different periods.

6. CONCLUSION

The study aimed to detect and identify frequency components that can help us diagnose faults related to rotor displacement in an induction motor. The research compared and analyzed eccentricity faults in a Three-phase induction motor. A FEM-based model is used to achieve the simulation of the induction motor. A 2D model was developed in Ansys and a simulation was run in a controlled environment to check on the results of a healthy motor and a faulty one with rotor displacement present in it. It is hard to replicate the rotor displacement in real-time to gather data, so simulations were taken into account for the practical implementation of this study. Finite element analysis and Fast Fourier transform analysis were done to get more precise results and graphs for the proper comparison. Magnetic flux distribution and saturation are plotted for each case by using Ansys Maxwell. A comparison is carried out between the FFT for currents to identify the different frequency components between healthy and faulty motors.

The FFT spectrum of the healthy and motor parameters shows that there are prominent frequency components present inside the faulty motor, which are not present in the case of a healthy one. These frequency components or eccentricity frequency components are present in the faulty case due to the rotor displacement and can be used to identify the fault present inside the motor. These simulation results were further analyzed in matlab to get a clear FFT spectrum and results. A comparison between these faulty frequency components between healthy and faulty scenarios is shown in table 5.1. The results have also been validated with the eccentricity equation to clarify it.

In future work, the entire simulation can be done by giving different load testing and varied fault conditions to check the effects of rotor displacement on the frequency spectrum of current. Using another software of more precise platforms will get an extra benefit in simulated results. Also, the model can be converted into a 3D model and compare the results with a real-time motor. Further signal analysis techniques can be carried out to help implement these findings in real-time scenarios to help prevent/detect faults related to rotor displacement.

SUMMARY

This thesis compares healthy and faulty induction motor to identify the reasons and factors that lead to air gap eccentricity. The distance between rotor and stator is equal for a healthy motor it could change because of particular reasons which lead to a defective motor.

Induction motors are the heart of the modern industry, which helps to convert electrical energy to mechanical energy through electromagnetic induction. Due to eccentricity fault in induction motors, many industries face maintenance shut down for a long time, which impacts productivity. This makes this topic is highly relevant in the modern era. The different methods for diagnosing faulty motors help to identify and prevent the consequences. The primary reasons include human error, environmental error, material error, design error etc.

The modeling and simulation of the induction motor was done using Ansys software. It was chosen because of its advantages, such as the construction of 2D and 3D design is more simple and realistic geometry than other software such as Cosmol, LabVIEW, Solidworks etc. The model was constructed with the help of the RMxpert tool. This model was converted into 2D and 3D model. Then the simulation was conducted until the machine remained steady for 3 sec and the collected data was imported as an excel file. Then the data is used in Matlab to get the FFT results. A matlab program was used to plot the frequency time domain for both models' current spectrum. The results graphs were generated as an output of the analysis such as induced current, induced voltages, moving torque, flux linkages, electrical and mechanical properties.

SUMMARY IN ESTONIAN

Käesolevas töös võrreldakse tervet ja vigast induktsioonimootorit, et selgitada välja põhjused ja tegurid, mis põhjustavad õhuvahe eksentrilisust. Terve mootori puhul on rootori ja staatori vaheline kaugus võrdne, kuid see võib muutuda teatud põhjustel, mis viivad vigase mootorini.

Induktsioonimootorid on kaasaegse tööstuse süda, mis aitab elektromagnetilise induktsiooni abil muundada elektrienergiat mehaaniliseks energiaks. Induktsioonimootorite eksentrilise vea tõttu seisavad paljud tööstusharud pikka aega hoolduse tõttu, mis mõjutab tootlikkust. Seetõttu on see teema tänapäeval väga oluline. Erinevad vigaste mootorite diagnoosimise meetodid aitavad tuvastada ja ennetada tagajärgi. Peamised põhjused on inimlik viga, keskkonnaviga, materjaliviga, projekteerimisviga jne.

Induktsioonimootori modelleerimine ja simulatsioon tehti Ansys tarkvara abil. See valiti selle eeliste tõttu, näiteks 2D- ja 3D-konstruktsioon on lihtsam ja realistlikum geomeetria kui teistes tarkvarades, nagu Cosmol, LabVIEW, Solidworks jne. Mudel konstrueeriti RMXprt tööriista abil. See mudel teisendati 2D- ja 3D-mudeliks. Seejärel viidi läbi simulatsioon, kuni masin püsis 3 sekundi jooksul paigal ja kogutud andmed imporditi excel-failina. Seejärel kasutati andmeid Matlabis FFT tulemuste saamiseks. Matlab-programmi kasutati mõlema mudeli praeguse spektri sageduse ajadomeeni joonistamiseks. Analüüsi väljundina genereeriti tulemuste graafikud, nagu indutseeritud vool, indutseeritud pinged, liikuv pöördemoment, vooluühendused, elektrilised ja mehaanilised omadused.

REFERENCES

- [1] J. Faiz, B. Ebrahimi ja M. Sharifian, „Different Faults and Their Diagnosis Techniques in Three-Phase Squirrel-Cage Induction Motors,“ *A Review, Electromagnetics*, kd. 26, nr 7, pp. 543-569, 2006.
- [2] M. M. Sedky, „Diagnosis of static, dynamic and mixed eccentricity in line start permanent magnet synchronous motor by using FEM,“ *International journal of electrical, robotics, electronics and communications engineering*, kd. 8, nr 1, pp. 29-34, 2014.
- [3] W. Zaabi, Y. Bensalem ja H. Trabelsi, „Fault analysis of induction machine using finite element method (FEM),“ *15th International Conference on Sciences and Techniques of Automatic Control and Computer Engineering (STA)*, pp. 388-393, 2014.
- [4] X. Liang, M. Z. Ali ja H. Zang, „Induction Motors Fault Diagnosis Using Finite Element Method: A Review,“ *IEEE Transactions on Industry Applications*, kd. 56, nr 2, pp. 1205-1217, 2019.
- [5] G. Mirzaeva ja I. S. Khalid, „Advanced diagnosis of rotor faults and eccentricity in induction motors based on internal flux measurement,“ *IEEE Transactions on Industry Applications*, kd. 54, nr 3, pp. 2981-2991, 2018.
- [6] A. Bouzida, R. Abdelli, O. Touhami ja A. Aibeche, „Dynamic eccentricity fault diagnosis in induction motors using finite element method and experimental tests,“ *International Journal of Industrial Electronics and Drives*, kd. 3, nr 4, pp. 199-209, 2017.
- [7] J. Faiz, B. Ebrahimi, B. Akin ja H. Toliyat, „Finite-element transient analysis of induction motors under mixed eccentricity fault,“ *IEEE transactions on magnetics*, kd. 44, nr 1, pp. 66-74, 2007.
- [8] A. Polat, Y. D. Ertuğrul ja L. T. Ergene, „Static, dynamic and mixed eccentricity of induction motor,“ *IEEE 10th International Symposium on Diagnostics for Electrical Machines, Power Electronics and Drives (SDEMPED)*, 2015.
- [9] V. Ghorbanian ja J. Faiz, „A survey on time and frequency characteristics of induction motors with broken rotor bars in line-start and inverter-fed modes,“ *Mechanical systems and signal processing*, kd. 54, pp. 427-456, 2015.
- [10] J. K. Kammoun, B. H. Naourez ja G. Moez, „Induction Motor under Eccentricity Fault based-on Finite Element Analysis,“ *4 th International Conference on Recent Advances in Electrical Systems*, p. 164, 2019.
- [11] J. Subramanian, S. Nandi ja T. Ilamparithi, „Detection and severity estimation of static and dynamic eccentricity in induction motors using finite element analysis,“ *2015 IEEE 10th International Symposium on Diagnostics for Electrical Machines, Power Electronics and Drives (SDEMPED)*, 2015.
- [12] H. N. Koti, H. Chen, Y. Sun ja N. A. Demerdash, „On Shortening the Numerical Transient in Time-Stepping Finite Element Analysis of Induction Motors Under Static and Dynamic Eccentricity Faults,“ *IEEE Energy Conversion Congress and Exposition (ECCE)*, pp. 3088-3095, 2019.
- [13] K. Prasob, N. K. Praveen ja T. Isha, „Inter-turn short circuit fault analysis of PWM inverter fed three-phase induction motor using Finite Element Method,“

- International Conference on circuits Power and Computing Technologies [ICCPCT]*, kd. 1, nr 6, 2017.
- [14] c. Vinothraj, T. B. Isha ja N. Praveen Kumar, „Bearing fault analysis in induction motor drives using finite element method,“ *International Journal of Engineering and Technology (UAE)*, kd. 7, nr 3, pp. 30-34, 2018.
- [15] A. Sapena-Bañó, F. Chinesta, M. Pineda-Sanchez, J. V. Aguado, D. Borzacchiello ja R. Puche-Panadero, „Induction machine model with finite element accuracy for condition monitoring running in real time using hardware in the loop system,“ *International Journal of Electrical Power & Energy Systems*, pp. 315-324, 2019.
- [16] A. Ghoggal ja A. H. Hamida, „Transient and steady-state modelling of healthy and eccentric induction motors considering the main and third harmonic saturation factors,“ *IET Electric Power Applications*, kd. 13, nr 7, pp. 901-913, 2019.
- [17] R. Sathish, R. Devarajan ja P. Ganga, „Analyzing and Detection of Rotor Faults in Squirrel Cage Induction Motor Drives Using MATLAB,“ kd. 4, nr 6, 2015.
- [18] R. Patole ja M. Bhagwat, „Detection of rotor and eccentricity faults in three phase induction motors using sound analysis,“ *International Research Journal of Engineering and Technology (IRJET)*, kd. 3, nr 7, pp. 1087-1089, 2016.
- [19] E. Ramaprasath ja P. Manojkumar, „Modelling and analysis of induction motor using LabVIEW,“ *International Journal of Power Electronics and Drive Systems*, kd. 5, nr 3, p. 344, 2015.
- [20] R. Gunabalan, S. Prabakaran, J. Reegan ja S. Ganesh, „Simulation of inverter fed induction motor drive with LabVIEW,“ *International Journal of Electrical and Computer Engineering*, kd. 8, nr 1, pp. 84-88, 2014.
- [21] P. K. N. ja I. T.B., „Electromagnetic field analysis of 3-Phase induction motor drive under broken rotor bar fault condition using FEM,“ *2016 IEEE International Conference on Power Electronics, Drives and Energy Systems (PEDES)*, pp. 1-6, 2016.
- [22] C. M. Apostoiaia, „Multi-domain system models integration for faults detection in induction motor drives,“ *IEEE International Conference on Electro/Information Technology*, pp. 388-393, 2014.
- [23] Z. Ferkova, „Comparison of two-phase induction motor modeling in ANSYS Maxwell 2D and 3D program,“ *2014 ELEKTRO*, pp. 279-284, 2014.
- [24] E. 4U, „Electrical 4U,“ 22 March 2021. [Võrgumaterjal]. Available: <https://www.electrical4u.com/wound-rotor-induction-motor/>. [Kasutatud 15 May 2022].
- [25] S. A. Alkadhim, „Three-phase Induction Motor: Types and Structure,“ 5 2020.
- [26] M. M. Rahman ja M. Uddin, „Online Unbalanced Rotor Fault Detection of an IM Drive Based on Both Time and Frequency Domain Analyses,“ 4 2017. [Võrgumaterjal].
- [27] K. Tian, T. Zhang, Y. Ai ja W. Zhang, „Induction Motors Dynamic Eccentricity Fault Diagnosis Based on the Combined Use of WPD and EMD-Simulation Study,“ 5 2018. [Võrgumaterjal].